Heritage Science

RESEARCH

Open Access

Original or post-war paintings? The fixed wooden scenery of the *Teatro Olimpico* in Vicenza: a guided multidisciplinary approach based on scientific analyses and HBIM

Fabrizio Antonelli[1], Rebecca Piovesan[1], Elena Tesser[1], Marco Tosato[2] and Emanuela Sorbo[2*]

Abstract

Archival resources, a photogrammetric survey, analysis of materials and techniques, and evaluation of the state of conservation were interconnected phases in the interdisciplinary research on the perspective scenery of the *Teatro Olimpico* in Vicenza. To fill existing gaps related to the history of this unique artefact and to the undocumented retouching of paint layers on the scenery during post-war reconstruction work, a broad analytical approach (optical microscopy, XRPD, SEM–EDX, μFTIR and μRaman) was applied to micro-samples, the selection of which was guided by consolidated geometrical and archival data. The aims were to obtain a characterisation of the pigments and binders and to evaluate the microstratigraphic sequence, the state of conservation of the scenery flats, and the deterioration processes involved. The findings unveiled a discernible variability in the production techniques of the finishes, frequently lacking the classic microstratigraphic sequence associated with the traditional method for painting on wooden panels from the sixteenth century. Moreover, by identifying many pigments that could be used as temporal markers we were able unequivocally to establish, for the first time, that a significant part of the scenery designed by the architect Vincenzo Scamozzi was heavily repainted in the post-WWII period. These analytical results and all the data collected on the artefacts over time were related through an HBIM model, enabling the historical and technical-analytical information to be linked to the geometrical survey and thus to provide guidance for actions based on current and future knowledge for the maintenance and monitoring of the *Teatro Olimpico*.

Keywords Wood painting, Renaissance theatres, Andrea Palladio, Vincenzo Scamozzi, Repainting, HBIM

Introduction

The *Teatro Olimpico* in Vicenza is the oldest, permanent indoor theatre of the modern era, designed by Andrea Palladio in 1580. Vincenzo Scamozzi designed the fixed wooden flats for the stage scenery in 1585. Today, these represent an *unicum* of the Renaissance era (Fig. 1). After they reassembled the scenes in 1945, restoration work was carried out on the pictorial layers and supports [1, 2], operations of which there is little documentation remains in the archives of the Soprintendenza of Verona. The first survey campaigns began in 1996 [1, 2] aimed at ascertaining the state of conservation of the theatre and the wooden scenery [3–7]. However, original and restoration elements were not clearly and analytically distinguished at the time. This is fundamental since the complex (chemical and mineralogical) composition of the paint layers of artworks can be linked to many factors, such as

*Correspondence:
Emanuela Sorbo
esorbo@iuav.it
[1] LAMA - Laboratory for Analysing Materials of Ancient origin, Department of Architecture and Arts, Università Iuav di Venezia, Calle della Laca, San Polo 2468, 30125 Venice, Italy
[2] Department of Architecture and Arts, Università Iuav di Venezia, Tolentini, Santa Croce 191, 30135 Venice, Italy

1. Archivio Fotografico Storico della Soprintendenza Archeologia, Belle Arti e Paesaggio per le provincie di Verona, Rovigo e Vicenza, b. Vicenza-Teatro Olimpico, Cartella II, 1944, 1944-05-07_7360_ cat.00600350_inv. VI ST 2118

2. State of the art photography of the central scene of scamozzi perspectives, Università Iuav di Venezia, 2023

3. Isometric visualization of the photogrammetric point-cloud, Università Iuav di Venezia, 2023

Fig. 1 Evaluation of iconographic-archival data: relationship between the condition of the scenery in its current state via laser scanner (lower portion) and comparison with the same portion of the items as photographed in 1944, before they were dismantled, (left photo) and the same viewpoint repurposed in 2023 (right photo). The lower image shows five of the seven streets of Thebes (17 single flats in total) the painting technique, the formation of decay products, including those associated with the environment, and the effect of past conservation operations. This characterisation is extremely useful for detecting historical events and improved understanding of the artistic heritage [8–11].

In this context, in order to develop a conservation project for Scamozzi's scenery, it was necessary to adopt a multidisciplinary approach which combined archival documentation and further data acquisitions, enabling a global understanding of the materials and their history, together with controlled and accessible storage of the documents produced. For this reason, this research proposes a dual approach to knowledge, both technical-analytical and historical-documentary, as advised by the international Burra Charter [12].

This dual approach involved a detailed scientific investigation of materials, guided by archival information, in order to enhance what had been partially investigated and to support the documentary study. Paintings on wooden supports have been widely studied in cultural heritage [13–17]. The preciousness of the materials and their small dimensions have often led to the use of non-destructive investigation techniques of various kinds [18–24]. In the specific case of the *Teatro Olimpico*, the areal extent of the artwork and the presumption of a very complex pictorial history resulted in a preference for a classic study of materials carried out through micro-sampling and laboratory analysis.

In addition, a method was developed to include, in a single organised work space, the data resulting from: (i) the study of documentary and iconographic sources conserved in the archives of the Soprintendenza of Verona; (ii) the investigation of previous cognitive campaigns conducted on the building; (iii) the recent photogrammetric survey of the scenery, which allows the simultaneous acquisition of geometric and radiometric data [25]; and (iv) the current analytical study of selected micro samples. The project found direct application within the HBIM (Heritage Building Information Modelling) environment [26], generating an interoperable and updatable model that links information and documents of a multidisciplinary nature to the geometric element. The HBIM makes it possible, for example, to date the dismantling and reassembly of the wooden scenery in order to understand and date restoration and conservation operations and to identify the materials studied through specific analytical investigations, linking them to the final reports. Moreover, the HBIM environment offers the opportunity to plan future actions and to monitor or define necessary investigations in a regime of controlled maintenance. The multidisciplinary approach adopted proved to be fundamental for correct planning of the survey of materials and the maximisation and validation of the information obtained through the coherent interpretation of the scientific data obtained. The integrated analysis of interdisciplinary and multidisciplinary skills (historical-archival survey, scientific laboratory investigation and HBIM) allowed the results to be read in an organic and interconnected way, and interpretation of the data to be raised to a higher level.

Materials and methods

The object of the study

Vincenzo Scamozzi designed the scenery for the *Teatro Olimpico* in Vicenza in 1585 for the first staging of *Oedipus Rex* [3, 27–31].

The installation consists of seven sets of flats made of wood with gypsum-based finishes, representing the seven streets of Thebes, arranged radially from the centre of the stage and constructed using the perspective technique. They therefore provide a section both in plan and elevation that narrows toward the perspective vanishing point. This peculiar construction typology meets the demands of perspective by adopting a ground plan in which the flats on either side of the street scene draw closer to each other as the street appears to lengthen, and also by reducing the height of the flats and the buildings they depict as the eye is drawn towards the end of the street.

According to archival documentation in the Soprintendenza of Verona,[1] the flats were dismantled during World War II, and the theatre's mobile decorative apparatus was moved to a safe location to preserve it from possible damage caused by the bombing of 1944.[2] After the end of the war, reassembly operations began in November 1945[3],[4] and the restoration begun then has continued, off and on, to the present day. Bibliographic

[1] Monumental Archive of the Soprintendenza Archeologia, Belle Arti e Paesaggio for the provinces of Verona, Rovigo and Vicenza (MASVRV), b. 116 "Vicenza-Teatro Olimpico", ff. 84/a-84/I

[2] MASVRV, b. 116 Vicenza-Teatro Olimpico, f. 84 «1944—Disassembly of scenes; Anti-aircraft protection; Cost estimate for the transport of the scenes and assembly» (in Italian: «1944—Smontaggio scene; Protezione antiaerea; Preventivo di spesa per il trasporto delle scene e montaggio»), Letter from Ferdinando Forlati, 4 May 1942.

[3] MASVRV, b. 116 Vicenza-Teatro Olimpico, f. 84 «1944—Disassembly of scenes; Anti-aircraft protection; Cost estimate for the transport of the scenes and assembly», cost estimate for the transport and relocation of the scenes of the Teatro Olimpico in Vicenza» (in Italian: «1944—Smontaggio scene; Protezione antiaerea; Preventivo di spesa per il trasporto delle scene e montaggio, preventivo di Spesa per il trasporto e ricollocazione in opera delle scene e del Teatro Olimpico di Vicenza»), 23 July 1945;

[4] MASVRV, b. 116 Vicenza-Teatro Olimpico, f. 84 «1944—Disassembly of scenes; Anti-aircraft protection; Cost estimate for the transport of the scenes and assembly» (in Italian: «1944—Smontaggio scene; Protezione antiaerea; Preventivo di spesa per il trasporto delle scene e montaggio»), Letter from Ferdinando Forlati, November 1945;

research revealed that restoration during the post-war reassembly operations involved the removal of 19th-century pictorial film [1]. In addition, the 1979 interventions on the wooden set focused on fixing the film, cleaning, plastering, and supplementing the pictorial pigments [2]. No information regarding the materials used in the various restoration operations is to be found in the archive documents.

From 1996 until 2009, thanks to the collaboration of several institutions (*Istituto Centrale per il Restauro-ICR*, *Centro Internazionale di Studi di Architettura Andrea Palladio-CISA*, Municipality of Vicenza and *Università Iuav di Venezia*/Laboratory for Analysing Materials of Ancient origin-LAMA), several campaigns of investigations were conducted on the theatre mainly to verify the state of conservation of wood components [3–7].

The preliminary investigation conducted in 2006 on the paint finishes of the fronts of flats 3B, 3D, and 5B, which is unpublished and not open access, was carried out through optical microscopy (in reflected, transmitted and UV light), X-Ray powder diffraction and Scanning Electron Microscopy and energy dispersive X-ray spectroscopy analyses. It indicates a paint palette that includes ochre (red, yellow, brown, and also raw umber), carbon black, white lead, lithopone, titanium white, barium white, rare green earth, and chromium oxide. The observed stratigraphy is straightforward, with few (maximum 4) paint layers applied on gypsum-based preparations that sometimes contain pigments such as carbon black and ochre. The presence of binders of a generic organic nature is occasionally noted, as is the presence of homogenization layers without aggregate and always of an organic nature. Additionally, very thin layers based on titanium oxide and/or barium sulphate are frequently found. The investigations conducted present the reported data without providing an interpretation at a global or stratigraphic level (other than the indication of some of the more recent pigments).

Information management and reading resource

In 2021, both topographic and laser scanning surveys of all portions of the theatre were carried out to generate the geometric consistency of the existing proscenium and wooden scenes [25]. The resulting data, optimised by the multiple techniques applied, have been processed to obtain an HBIM model of portions of the Theatre. BIM is the digital information system for the construction of a building consisting of a 3D model integrated with physical data from multiple disciplines (architectural, physical, installation, structural, etc.). Today, BIM models applied to Built Cultural Heritage (HBIM) [32] allow the inclusion of abundant geometric-type information [33] as well as data referring to the construction techniques and history of the building, its state of preservation and the materials employed [26, 34–37]. As is necessary when working within the HBIM environment, the 3D model was progressively simplified [38] and the scenery was modelled by sector without detailing the development of the decorative apparatus. The theatre was subdivided into macro-elements (i.e., perspective scenery, proscenium, orchestra, cavea, roofing, odeum, antiodeum, elevations, garden) to which information of both a historical–critical and scientific nature could be attached, as well as future possible operational guidelines. In this way, the efficacy of the restoration work can be simply managed and monitored.

The archival, bibliographic and iconographic information acquired during the document search was subdivided by type and stored in a digital repository, as illustrated (Fig. 2). In addition to the source type, another element of file subdivision was the date of data acquisition or document creation. In the case of archival sources, these were sorted by date of document creation, thus year by year until 2020. Case study analyses were sorted by the date of information acquisition.

The architecture of the information repository allows for correspondence between the sources and the three-dimensional element within the HBIM environment. The data collected, whether historical, technical, analytical or geometric, were all linked within the 3D model. The HBIM models can support different types of analysis in a single digital model [39] and can be continuously updated [40]. By interrogating a three-dimensional element in the HBIM model, it is possible to retrieve differentiated types of information. Some can be experienced by the user immediately, such as scenery construction date, architect or ongoing analysis. Others, such as the final reports of investigations performed in previous data acquisition or photographic campaigns, are connected through dynamic links directly available in the model. The following information has been linked to each element in the HBIM: dating, author, transformations, materials, construction characteristics, state of preservation, investigations carried out, studies to be carried out, historical iconography, photographs, critical issues, action to be taken.

In particular, the model used made it possible, through the interpolation of historical and analytical information, to guide the new investigations that are the subject of the current research, orienting the sampling campaign towards the areas that had been less analysed. Thanks to the HBIM model, it was possible to make a direct comparison between the previous survey campaigns (mineralogical-petrographic and physical–mechanical), and it emerged that the most significant ones were carried out between 2006 and 2009 and concerned flat 1

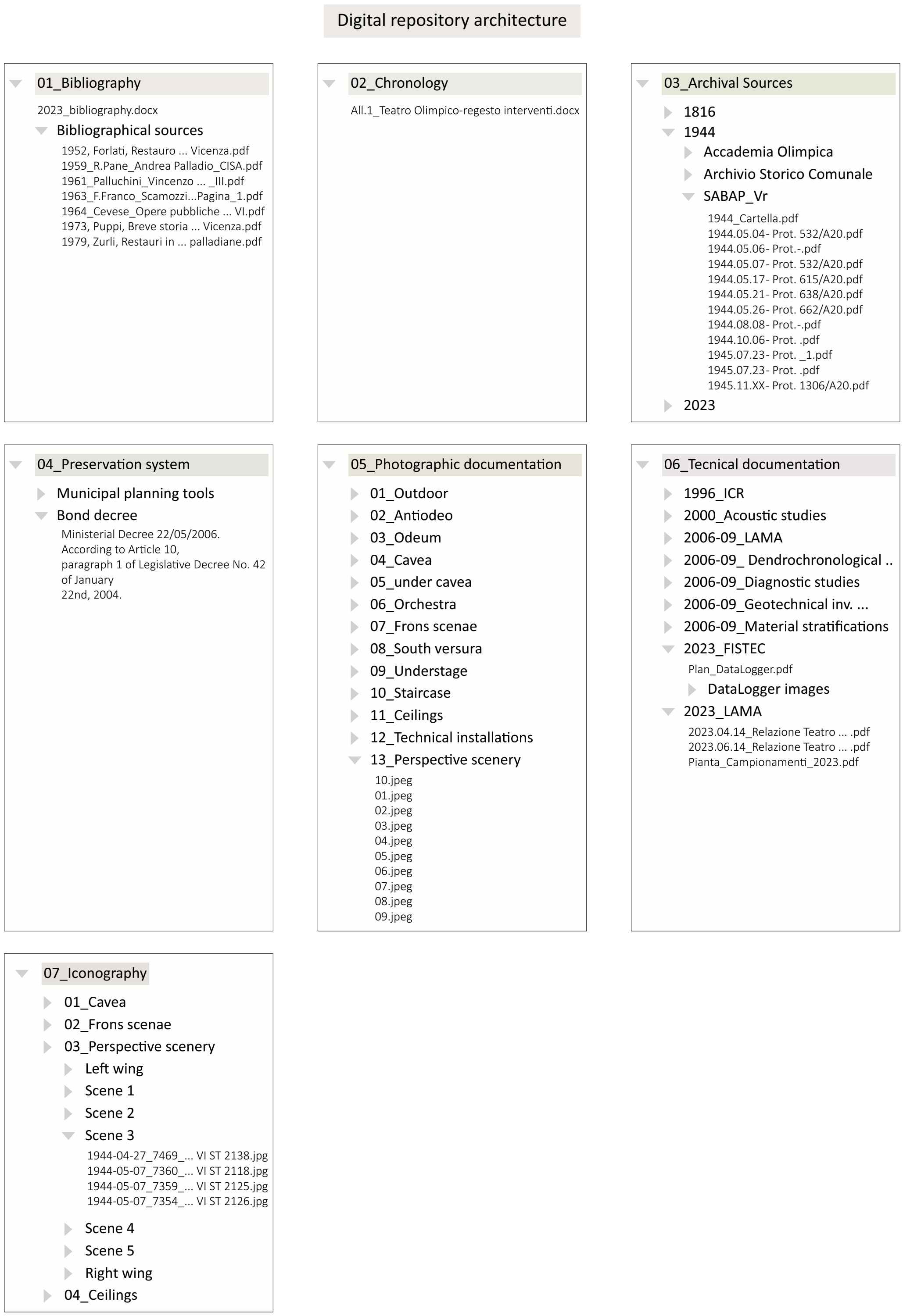

Fig. 2 Structure of the digital repository for cataloguing information related to the *Teatro Olimpico*

(front 1B), flat 3 (fronts 3B, 3C and 3E) and flat 5 (front 5A), the upper part of the scenery representing the sky, the cave roof, the odeon, the sub-scene and proscenium areas [7]. To evaluate the state of conservation of the fronts, the survey orthophotos were compared with historical photographs conserved in the Archives of the

Soprintendenza of Verona and taken during the disassembly phases in 1944, which provide an accurate picture of the state of conservation of the paint surfaces in the post-war period. Critical evaluation of the historical images extended our knowledge of the historical state of preservation of the building through mapping the ancient pictorial layers and their state of conservation. This methodology gave specific indication of the areas needing to be sampled during the present research [41]. The samples taken in the previous campaigns were mapped (for the first time) in the elevations of the wooden flats and linked to the HBIM model to obtain a complete framework of preliminary knowledge of the materials of the stage flats and their state of preservation. This made it possible to orient the new samples to be taken from flat 1 (frontal areas 1A and 1B), flat 2 (frontal areas 2B and 2C) and flat 3 (frontal areas 3A, 3B and 3C) (Fig. 3).

The HBIM model also allowed for the inclusion of other investigations carried out in previous campaigns, such as structural diagnostics in the sub-scene spaces; endoscopic investigations in the walls and sub-scene; magnetometric and thermographic investigations in the proscenium, in the ceiling above the stage scenery, painted to depict the sky, and the ceiling over the cavea and the Odeum, highlighting the fact that the theatre's internal microclimatic parameters had never previously been monitored. These investigations commenced recently in order to gather data on the fluctuations in internal temperature and relative humidity, as well as to establish possible correlations between these factors and the development of deterioration phenomena or pathologies on surfaces or structures. In addition to microclimatic investigations, acoustic monitoring was carried out to verify the response to acoustic stresses of the interior spaces of the Theatre, which serves as a sounding board. It is currently being determined whether the structural alterations made during the second half of the twentieth century may have impacted the acoustic and microclimatic behaviour of the interiors of the Theatre.

The HBIM model makes it possible to have a diachronic and overall reading of the events and analyses of each of the theatre's architectural elements organised in a multi-scalar manner (from the flat to the individual sample). Moreover, by being able to integrate past and current investigations, it is a useful way of monitoring the effectiveness of protection and conservation actions, both those already conducted and those in progress ("Three-dimensional model data visualisation and cataloguing for preservation" section explains what information is available in the model when an item is selected).

In the present work, micro-invasive sampling (all samples taken measure a millimetre at most) was carried out with a view to characterising the pictorial finishes of the wooden flats, taking into account the chromatic variability of the decorations. The most characteristic and repetitive colours were therefore sampled in significant numbers from each of the most important flats, as indicated by the study of archival resources. Sampling was performed on portions that were already damaged and/or hidden so as to avoid affecting the aesthetics of the scenery in any way or damaging the paintings further; in all, fourteen micro samples were collected from the flats. Table 1 contains a complete list of the collected samples, while Fig. 3 shows the path followed by the research team in building the HBIM model so as to understand where the new samples have to be taken from. The starting point of the process was the point cloud obtained in the laser scanning campaign, which was necessary for construction of the model (column 1), but more important was the comparison between the survey and archival documents related to the previous campaigns and historical photos of the reassembly of the scenes. These three elements visualized simultaneously in the HBIM made it possible to locate where new sampling should take place, avoiding repetitions, overlaps or disadvantageous locations. Figure 3 is also a static representation of the dynamic path of the research, from which it is clear how the model can be used for research purposes: the first column shows the archival sources used to gather information about the historical development of the building and the restorations to which the *Teatro Olimpico* was subjected in the past; the second column shows the recent history of the scenery, specifically the past analytical campaigns; the third column displays the location of all the sampling points of surface film and pictorial materials carried out on the 3A front during the ongoing research project. For the purpose of the representations in Fig. 3, the flats have been virtually dismantled to pinpoint previous survey locations and to highlight comparison with the new process of analytical survey methods using HBIM.

Analytical methods

The samples were investigated using a multi-analytical approach to define their stratigraphy accurately and identify their composition in terms of binders and pigments. A polished cross-section was prepared for each sample by embedding it in epoxy resin. Polishing was performed dry and/or using petroleum as a fluidifying agent to avoid any hydrosoluble material (e.g., gypsum) being in contact with water. Where necessary, certain analyses were conducted directly on the materials as they were. The analytical methods adopted are summarised below.

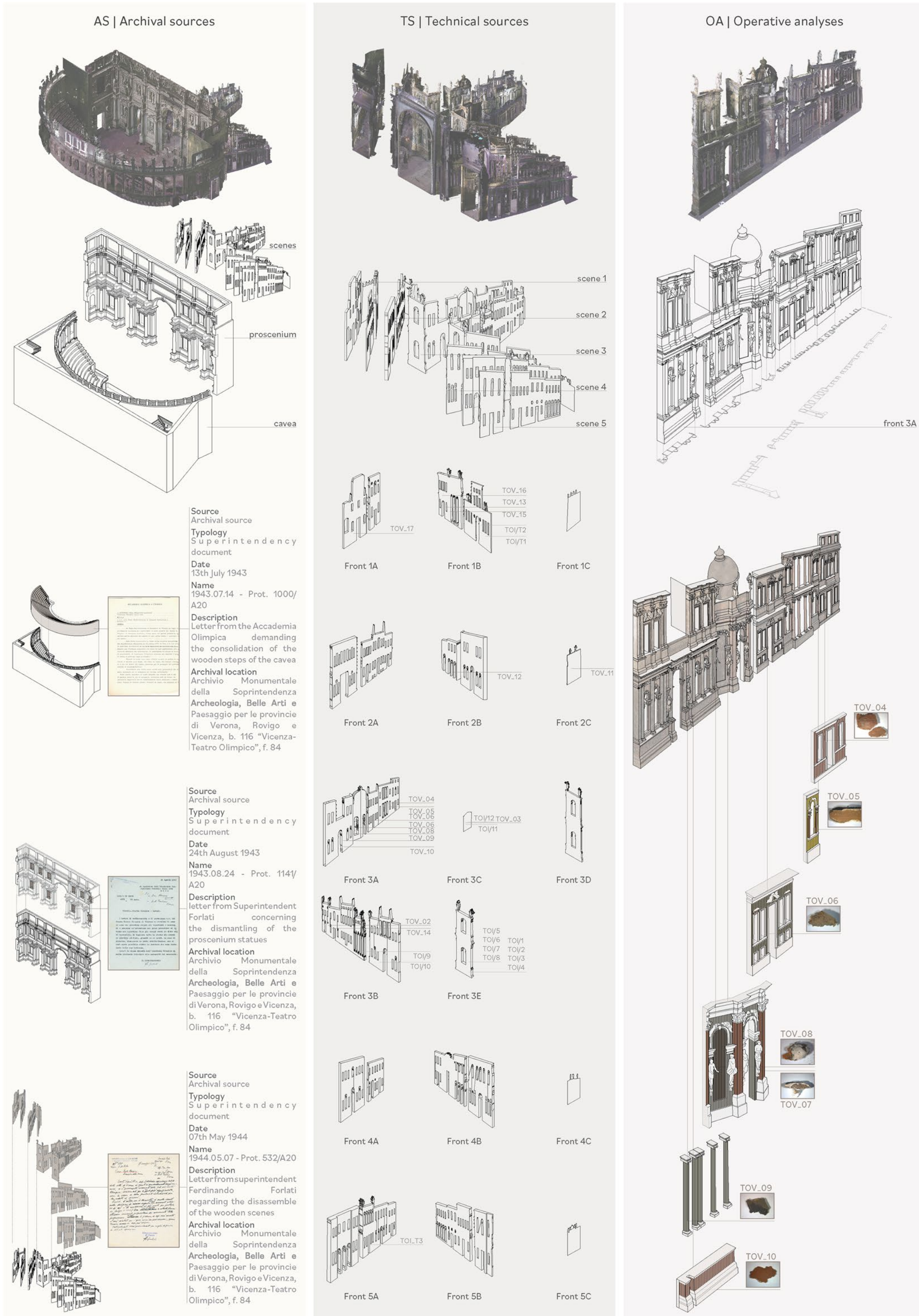

Fig. 3 Static visualization of the dynamic path of research: the first column shows archival sources; the second column shows past analytical campaigns; the third column shows the location of all points where photographs and samples of pictorial materials were taken on the 3A front during the current research project. The image highlights comparison with the new process of analytical survey methods through the use of HBIM

Table 1 List of samples taken from the fixed wooden scenery of the *Teatro Olimpico* in Vicenza

Sample name	Flat	Sampling location	Material	Colour	Analyses
TOV_02	3C	Near an existing lacuna at the upper right end of the first architectural module, to the right of the second oval element (oval window)	Fragment of black-brown paint with underlying grey-white preparation	Brown-black	RLOM; XRPD; SEM–EDX; µRaman; µFTIR
TOV_03	3C	From the capital of the second frontal column to the left, near a lacuna	Fragment containing a complete stratigraphy from the light and dark brown paint film to the underlying wood	Light and dark brown	RLOM; XRPD; SEM–EDX; µRaman; µFTIR
TOV_04	3A	Near the end of the flat. A sample of finishing layer was taken in the lower register of the front, at the top left of the second-to-last opening. Found woodworm holes	Fragment of red paint and underlying white preparation	Red	RLOM; XRPD; SEM–EDX; µRaman; µFTIR
TOV_05	3A	Near the closure of the street scene, particularly in the last "building." A finishing layer sample was taken to the right of the supporting column of the arched opening in the lower register of the front	Fragment of yellow-ochre coloured filler of a lacuna and white preparation	Yellow	RLOM; XRPD; SEM–EDX; µRaman; µFTIR
TOV_06	3A	In the centre of the street scene, particularly in the third building. A sample of finishing layer was taken in the lower register of the front, between the door and the first pair of windows on the left	Fragment of brown-green finishing layer	Brown-green	RLOM; XRPD; SEM–EDX; µRaman; µFTIR
TOV_09	3A	At the beginning of the street scene, in the first building characterized by the presence of columns. A sample of finishing layer was taken in the lower register of the front, in the first column to the right of the door	Green decoration in imitation of *Verde Antico* marble. Fragment of green and brown polychrome finishing layer	Green & brown	RLOM; XRPD; SEM–EDX; µRaman; µFTIR
TOV_10	3A	At the beginning of the street scene, in the first building characterized by the presence of columns. A finishing layer sample was taken in the lower register of the front, specifically in the basement plinth at the first niche to the right of the door. Previous detachment	Fragment of orange-red finishing layer	Orange	RLOM; XRPD; SEM–EDX; µRaman; µFTIR
TOV_11	2C	From the second column on the left looking at the painted statue	Fragment of beige finishing layer	Beige	RLOM; XRPD; SEM–EDX; µRaman; µFTIR
TOV_12	2B	From the trifora (first arch towards the proscenium, left-hand column)	Fragment of brown finishing layer	Brown	RLOM; XRPD; SEM–EDX; µRaman; µFTIR
TOV_13	1B	From the back of the flat	Splinter of wood with grey deposit	–	RLOM; XRPD; SEM–EDX; µRaman; µFTIR
TOV_14	3B	From the back of the flat	Splinter of wood with grey deposit	–	RLOM; XRPD; SEM–EDX; µRaman; µFTIR
TOV_15	1B	At the end of the street scene. From the green column (the first from the bottom) adjacent to the statue	Fragment of green finishing layer	Green	RLOM; SEM–EDX; µRaman; µFTIR
TOV_16	1B	From the back of the flat	Splinter of wood	–	RLOM; XRPD; SEM–EDX; µRaman; µFTIR
TOV_17	1A	At the beginning of the street scene, from the fourth reproduction marble slab in imitation of *Fior di Pesco* variety, after the second opening from the proscenium	Fragment of ochre-coloured paint	Yellow ochre	RLOM; XRPD; SEM–EDX; µRaman; µFTIR

Reflected light optical microscopy (RLOM)

Reflected light optical microscopy was adopted on polished cross-sections to investigate, describe and measure the microstratigraphy of the layers and identify their various components (pigments, binder). This study also used ultraviolet light (UV) observation to estimate the fluorescence induced by any organic substances. For this purpose, use was made of a Leica DM2500 optical microscope equipped with a mercury vapour lamp and a set of filters suitable for visualising the fluorescence emission response (green emission: excitation filter BP 450–490 nm, dichroic mirror FT 510 nm, emission filter LP 515 nm; blue emission: BP 320–380 nm, dichroic mirror FT 400 nm, emission filter LP 425 nm).

X-Ray powder diffraction (XRPD)

Mineralogical analyses were performed by X-ray powder diffraction on fine-grained powder samples (obtained with an agate mortar and pestle) using a Panalytical Empyrean diffractometer, operating at 40 kV and 40 mA, in Bragg–Brentano reflection geometry and equipped with CuKα radiation and an X'Celerator detector. Qualitative diffraction data analysis was carried out with X'Pert HighScore Plus® software (PANalytical) and the PDF-2 database. The reference intensity ratio (RIR) method, rather than only the intensity of the peak channel, was used to semi-quantify the amount of the recognised materials in the multiphase XRPD patterns. This analysis was carried out, where possible, on single layers or several together as long as they could be separated manually with the support of the stereomicroscope and scalpel.

Scanning Electron Microscopy and energy dispersive X-ray spectroscopy (SEM–EDX)

Micro-morphological, textural and elemental compositional investigations were carried out using a ZEISS EVO15 scanning electron microscope (SEM) equipped with a LaB6 cathode coupled with an X Flash 6160 BRUKER energy-dispersive X-ray spectroscopy (EDX) system, on platinum-coated cross-sections. A series of analyses was performed on each recognised layer to characterise the different materials and measure the thickness of the layer where possible. Elemental maps were also generated to enhance comprehension of the samples' multilayer structure.

Micro-Raman spectroscopy (μRaman)

Micro-Raman spectroscopy was performed with a DXR2 Thermo Scientific™ Raman microscope, equipped with two frequency-stabilised single-mode diode depolarised lasers at 785 nm and 532 nm. Spectra were acquired on the cross-sections, using laser power varying between 1 and 30 mW for the 785 nm laser and between 1 and 10 mW for the 532 nm laser. Spectrograph aperture of 25 μm pinhole and 10X and 50X objectives were also adopted, therefore with a spectral resolution in the range 2.7–4.2 cm^{-1} and a spatial resolution of 2.1 μm. Here too, a series of pinpoint analyses was performed on recognised layers and coloured particles to characterise the different materials and pigments where possible.

Fourier-transform infrared spectroscopy (μFTIR)

The identification of the organic compound was performed using a Thermo Scientific™ Nicolet™ iN10 MX Infrared Imaging Microscope for pinpoint analysis of both the cross-sections and the untreated samples. In the latter case, a small amount of powder sampled from every layer identified by stereomicroscope was taken using a needle, then deposited and pressed on a standard KBr pellet for each micro-fragment. The analyses were performed in transmittance mode, with the minimum spectral resolution equal to 1 cm^{-1} and 60 consecutive scans. In addition, fingerprint peaks were mapped on cross-sections using germanium crystal micro-tip ATR with 0.35 mm Ø for tapping-mode investigation of the component distribution in the microstratigraphy.

Field acquisition

A photogrammetric survey provided enhanced knowledge of the wooden flats and the theatre proscenium. The use of *Structure from Motion* software in processing photograms yields various outputs, including high-resolution textures and orthophotos. These outputs represent two-dimensional renditions of three-dimensional space, providing geometrically scaled and measurable representations [25, 42].

In the frame acquisition campaign, 964 shots of the central street scene were acquired. Due to difficulties encountered inside the theatre, such as poor lighting and insufficient space, the data were obtained partly with an action camera and partly with a Canon 5D Mark II, as described in Ballarin et al. [43]. In particular, 24 of the 964 frames were taken with the DJI Osmo Mobile 3 action camera at maximum resolution (4000 × 3000 px), and 940 with a Canon 5D Mark II coupled with Canon EF 24-70 mm F.4 IS II lens at full resolution (5616 × 3744 px). The frame capture was manual and supported by a soft LED box with variable colour temperature and illumination intensity to correct interior lighting conditions proactively. This expedient was adopted because the existing illumination caused strong contrasts of light and shadow, resulting in an almost complete loss of information in the darker portions.

The shots were processed using the commercial software Agisoft Metashape Pro. The photogrammetric model was oriented on the same reference system previously used for processing the topographic and laser scanning survey. The decision to use the same reference system was made for two main reasons: (i) the previous survey was already available to the research team, so it was not necessary to perform a new topographic survey; (ii) the use of a shared reference system opens up the possibility of including the results of the photogrammetric survey within the HBIM environment. Thus, it became feasible to link the photogrammetric point cloud to the pre-existing information model, employing the same reference system.

Results and discussion

Paint microstratigraphy

The microstratigraphic study of the pictorial finishes of the wooden scenery proved to be varied and sometimes very complex (Fig. 4). The analyses and observations conducted enabled the pigments, fillers and binders used to be identified and recurring sequences of layers exhibiting similar characteristics to be recognised and categorised. In the most successful cases, also thanks to the identification of specific pigments, it was possible to attribute a relative temporal collocation to the paint layers concerned in the series of restoration and/or retouching operations to which the flats have been subjected over the centuries.

In order to describe the microstratigraphy more efficiently, the layers identified were named alphabetically starting from the deepest layer (i.e., layer A) to the top (i.e., layer C for a sequence of 3 layers) (Table 2).

Wooden supports

The use of HBIM and the introduction of all prior investigations into its archival system prevented unnecessary repetition of characterizations, and enabled assessments to be based on these findings as regards the condition of finishes and supports. The study of the wooden supports, therefore, relies on outcomes from earlier investigations as revealed by archival research.

According to this research, Zurli was the first Superintendent to order the scenery to be studied during the 1979 restoration campaign [2]. His predecessor, Forlati, mentions the removal of "the nineteenth-century paintwork" to restore "the original paintwork" [1] during post-war restoration, but he makes no reference to investigations guiding the restoration efforts. The first evaluation of the condition of the theatre's wooden elements dates from 1996 when the ICR photographed various signs of aggression attributable to xylophagous insects and fungi (woodworm holes, wood decay) during an exploratory survey[5] supporting the development of a suitable fire-fighting system [6]. Between 2006 and 2009, CISA, in collaboration with the LAMA Laboratory (*Università Iuav di Venezia*) and the Municipality of Vicenza, conducted an investigative campaign to develop a conservation project for the *Teatro Olimpico* [7]. This campaign involved dendrochronological analyses to classify and date the wooden elements. Results achieved demonstrated that the wooden perspective flats were crafted from Silver Fir (*Abies Alba*) and Spruce (*Picea Abies*) and probably date between 1520 and 1539.[6] Lastly, in the report on the restoration work on the ceiling of flat 3, it is noted: "*Inspection of the front and back of the wooden structure does not, in fact, reveal the presence of* rodent teeth marks*…except for just two points, but the phenomenon as a whole appears to be of previous origin*"[7] [6, 44].

In the survey campaign described in this article, there was no repetition of investigations to characterize the wood and its state of preservation. Nonetheless, microstratigraphic analyses conducted on the three wood samples taken from the back of flats TOV_13, TOV_14 and TOV_16 confirm the presence of some woodworm holes and deposits of soft, brown rot [45].

In addition, all the analyses performed on the grey deposits recognised on the surface of samples TOV_13 and TOV_14 revealed the presence of gypsum residues. Moreover, a discontinuous yet cohesive layer consisting of sub-microcrystalline silica was also identified through XRPD, μFTIR, and EDS analysis, exhibiting abundant Si and O content (Fig. 5a). Perhaps this latter detail can be linked to the use of silicate-based products adopted to treat the backs of the flats, although their application on wood is not widely attested in the literature [46].

[5] MASVRV, b. 116 Vicenza-Teatro Olimpico, f. 84/D «1996—Calendar of events; Installation of dimmer cabinet; ICR—report on the state of conservation of the wooden structures; adaptation of the electrical installation; lighting system; project for a stair lift» (in Iitalian: «1996 – Calendario manifestazioni; Installazione armadio dimmer; ICR – relazione stato conservativo strutture lignee; adeguamento impianto elettrico; impianto illuminotecnico; progetto montascale», Istituto Centrale per il Restauro—ICR. Laboratory of Biological Investigations—entomology section. State of conservation of the wooden structures of Andrea Palladio's Teatro Olimpico in Vicenza (in Italian: Laboratorio di indagini biologiche – sezione di entomologia. Stato conservativo delle strutture lignee del Teatro Olimpico di Andrea Palladio in Vicenza), edited by Italo Tigliè , April–May 1996;

[6] MASVRV, b. 116 Vicenza-Teatro Olimpico, f. 84/G «2007—Performances; new academic charges; preliminary investigations and verifications for the design of restoration works—CISA Palladio» (in Italian: «2007 – Spettacoli; nuove cariche accademiche; indagini e verifiche preliminari alla progettazione di interventi di restauro – CISA Palladio»), Teatro Olimpico—surveys, investigations and analyses. Final report (in Italian: Teatro Olimpico – rilievi, indagini ed analisi. Relazione finale), 15 December 2006;

[7] MASVRV, b. 116 Vicenza-Teatro Olimpico, f. 84/I «2020—Teatro Olimpico: plan of investigations and conservative restoration of the Scamozzi scenes» (in Italian: «2020—Teatro Olimpico: piano d'indagini e restauro conservativo del cielo delle scene scamozziane»), October 2020;

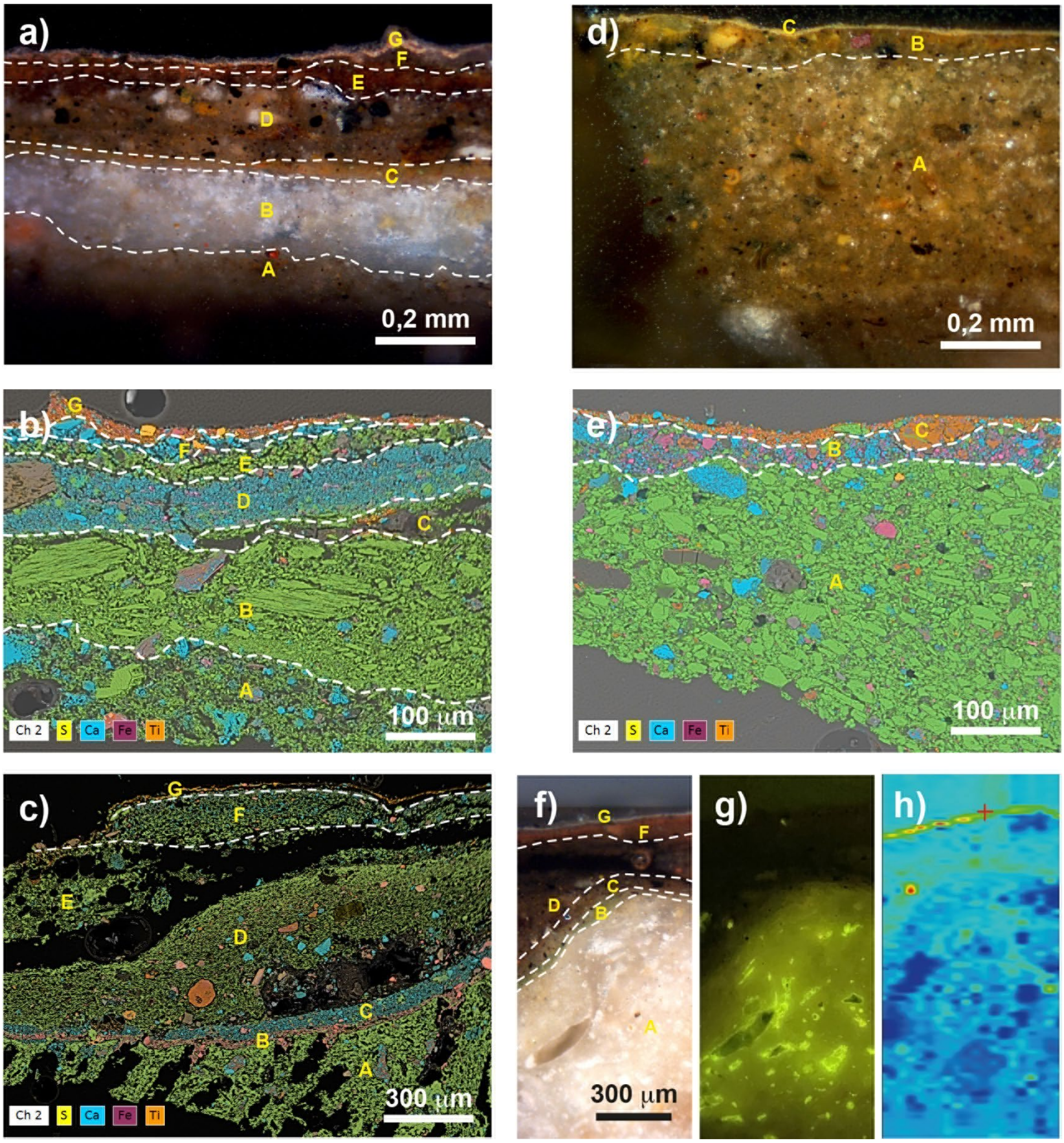

Fig. 4 Cross sections in reflected-light photomicrographs of samples TOV_02 and TOV_17 (**a**, **d**); elemental EDS maps in false colours of samples TOV_02, TOV_04 and TOV_17 (**b**, **c**, **e** respectively). Reflected-light (**f**) and UV green emission (**g**) photomicrographs of sample TOV_04 compared with µFTIR map (**h**) of the characteristic peak of acrylic polymers (ν C=O, carbonyl, 1730 cm.$^{-1}$)

Ground layers

Since at least the twelfth century, the recipe historically used for ground layers [47] involved gypsum or anhydrite as the inert material and animal glue, usually rabbit glue, as an organic binder. This mixture was laid on top of wood previously treated with strong glue and covered with a canvas soaked in glue, a procedure that offered excellent chemical stability. The ground layers might then be numerous, starting with coarse plaster mixtures and gradually decreasing in grain size. Finally, each ground layer underwent the *'rasatura'* procedure, i.e., its surface was levelled with a special tool to remove protrusions and to smooth the surface. Sometimes, this procedure was replaced for the final layers by applying a layer of glue on the last ground layer [47]. In the case of the *Teatro Olimpico*, although in some places there is a correspondence with the chemical and mineralogical composition of the preparation, no evidence of canvas has been found in the samples analysed. The basic composition of most of the ground layers (Fig. 4) found is calcium sulphate ($CaSO_4$), but in different degrees of hydration (often coexisting in the same sample) and

Table 2 Description, composition and thickness of each layer of the samples analysed

Sample	Layer	Description	Thickness (μm)	Results			
				Binder (§ Ground layers & Organic binders and retouching)	**Filler (§ Ground layers)**	**Pigments (§ Pigments)**	**Secondary products**
TOV_02	A	Grey 1st ground layer (type 1 in § Ground layers)	–	Anhydrite	Anhydrite, calcite		
	B	White 2nd ground layer (type 1 in § Ground layers)	200	Anhydrite, gypsum	Anhydrite, gypsum calcite, quartz		
	C	Colourless-transparent smoothing layer	20	Probably organic			
	D	Pale yellow 3rd ground layer sometimes double-layered (type 3 in § Ground layers)	90	Calcite, protein tempera	Calcite, gypsum, quartz	Red ochre, yellow ochre, green earth, carbon-based black	
	E	Brown/red paint layer	50	Gypsum, anhydrite	Gypsum, anhydrite, calcite	Carbon-based black, red ochre	
	F	Grey varnish layer	30	Probably organic	Calcite		
	G	Yellowish/brown finishing layer	15	Probably organic	Calcite	Carbon-based black, barium white, titanium white	
TOV_03	A	Wood substrate residues	–				
	B	Grey-brown paint layer	110	Gypsum, anhydrite, polysaccharide tempera, *probably, acrylic polymer*	Gypsum, anhydrite	Carbon-based black, red ochre, yellow ochre	
	C	Pale yellow finishing layer	15	Acrylic emulsion		Barium white, titanium white	
TOV_04	A	White 1st ground layer (type 1 in §Ground layers)	–	Gypsum	Gypsum, calcite, quartz	Carbon-based black	Weddellite
	B	Green/blue paint layer	90	Gypsum		Green earth, carbon-based black, yellow ochre	
	C	Yellow/grey 2nd ground layer (type 3 in § Ground layers)	50	Calcite	Calcite, gypsum	Yellow ochre, red ochre, carbon-based black	
	D	Yellow/grey 3rd ground layer (type 2 in § Ground layers)	430	Gypsum	Calcite, gypsum, quartz	Carbon-based black, yellow ochre, red ochre	Weddellite (traces)
	E	Orange paint layer	80	Gypsum	Gypsum	Carbon-based black, yellow ochre, red ochre	
	F	Yellow/orange paint layer	55	Gypsum, anhydrite, acrylic polymer	Gypsum, anhydrite, calcite	Carbon-based black, yellow ochre	
	G	Pale yellow finishing layer	10	Probably organic	Anhydrite	Yellow ochre, red ochre, barium white, titanium white	

Table 2 (continued)

Sample	Layer	Description	Thickness (μm)	Results			
				Binder (§ Ground layers & Organic binders and retouching)	**Filler (§ Ground layers)**	**Pigments (§ Pigments)**	**Secondary products**
TOV_05	A	Brown 1st ground layer	–	Gypsum, anhydrite, acrylic polymer	Gypsum, anhydrite, calcite	Carbon-based black, yellow ochre, red ochre	Weddellite
	B	White 2st ground layer	1440	Calcite, acrylic polymer	Calcite		Weddellite (traces)
	C	Yellow paint layer	40	Calcite, acrylic polymer	Calcite, gypsum	Yellow ochre, barium white, titanium white	
TOV_06	A	Brown/green paint layer	–	Gypsum, acrylic polymer	Gypsum, calcite	Yellow ochre, chromium oxide	Weddellite
	B	White/orange ground layer	110	Calcite, acrylic polymer	Gypsum, anhydrite, calcite, dolomite, quartz	Carbon-based black	Weddellite
	C	Whitish finishing layer	15			Titanium white	
TOV_09	A	White 1st ground layer (type 1 in § Ground layers)	–	Gypsum, anhydrite, acrylic polymer	Gypsum, anhydrite, calcite, quartz		
	B	Red paint layer	60	Gypsum, acrylic polymer	Gypsum	Red ochre, lead sulphate	
	C	Colourless-transparent smoothing layer	20	Probably organic			
	D	Orange paint layer	65	Probably organic	Calcite	Red ochre	
	E	White paint layer	30	Gypsum, probably organic	Gypsum	Dolomite, lead sulphate	
	F	Yellow translucent 2nd ground layer (type 2 in § Ground layers)	100	Gypsum, probably organic	Gypsum	Yellow ochre	
	G	Grey/brown translucent (on the right) paint layer	60	Gypsum, probably organic	Gypsum, calcite	Carbon-based black, indigo, red ochre, titanium white	
	H	Grey/green translucent (on the left) paint layer	25	Gypsum, anhydrite, acrylic polymer	Gypsum, anhydrite, calcite	Carbon-based black, indigo, titanium white, lead sulphate	
	I	White finishing layer	10	Probably organic	Calcite	Titanium white	
TOV_10	A	Grey 1st ground layer (type 2 in § Ground layers)	–	Gypsum	Gypsum, calcite		
	B	Yellow/green paint layer	80	Anhydrite, gypsum (polystyrene from the support)	Anhydrite, gypsum	Green earth, red ochre, yellow ochre	
	C	Yellow/green paint layer	25	Gypsum, anhydrite	Gypsum, anhydrite, quartz	Red ochre, yellow ochre, carbon-based black	
	D	Grey translucent 2nd ground layer (type 2 in § Ground layers)	280	Anhydrite, gypsum, acrylic polymer	Anhydrite, gypsum	Yellow ochre, carbon-based black	
	E	Orange paint layer	35	Acrylic polymer, gypsum, anhydrite	Gypsum, anhydrite	Carbon-based black	
	F	Transparent varnish layer	20	Probably organic	Calcite	Yellow ochre, barium white	

Table 2 (continued)

Sample	Layer	Description	Thickness (μm)	Results			
				Binder (§ Ground layers & Organic binders and retouching)	Filler (§ Ground layers)	Pigments (§ Pigments)	Secondary products
TOV_11	A	Wood substrate residues	–				
	B	White/grey 1st ground layer	160	Gypsum, anhydrite, calcite, acrylic polymer	Gypsum, anhydrite	Yellow ochre	
	C	White paint layer	30	Acrylic polymer, gypsum, anhydrite	Anhydrite, gypsum, calcite, quartz	Titanium white, barium white, carbon-based black	
TOV_12	A	Grey 1st ground layer (type 2 in § Ground layers)	–	Gypsum	Gypsum, calcite, quartz	Carbon-based black, red ochre	
	B	Yellowish/brown 2nd ground layer (type 2 in § Ground layers)	1640	Gypsum, anhydrite	Gypsum, anhydrite	Red ochre, yellow ochre, carbon-based black	Weddellite
	C	White paint layer	20	Acrylic polymer, gypsum	Gypsum, calcite, quartz	Titanium white, barium white, yellow ochre	
TOV_13	A	Wood	–				
	B	Grey deposit	0–200	Gypsum, amorphous silica			
TOV_14	A	Wood	–				
	B	Grey deposit	0–50	Gypsum, amorphous silica			
TOV_15	A	Wood substrate residues	–				
	B	Grey 1st ground layer	120	Gypsum	Gypsum	Yellow ochre, carbon-based black	
	C	White/grey paint layer	25			Titanium white, barium white	
TOV_16	A	Wood	–				
TOV_17	A	Yellowish ground layer (type 2 in § Ground layers)	–	Gypsum, anhydrite	Gypsum, anhydrite	Carbon-based black, yellow ochre	
	B	Yellow paint layer	60	Gypsum, probably organic	Gypsum, calcite, dolomite, quartz	Red ochre, yellow ochre, carbon-based black	Weddellite
	C	White paint layer	10	Acrylic polymer, gypsum	Gypsum	Titanium white, barium white, chromium oxide	

Since it is not possible to be certain that the deepest layer (i.e., layer A) has been sampled in its totality, the thickness of this layer will not be reported

thus in different mineralogical phases, from anhydrite ($CaSO_4$) to bassanite ($CaSO_4 \bullet \frac{1}{2}H_2O$) to gypsum ($CaSO_4 \bullet 2H_2O$). Anhydrite is a mineral (naturally available or synthetically produced by calcinating gypsum) which, in the presence of water, hydrates and transforms into gypsum. Thanks to this characteristic, it also serves as an inorganic binder, and is typically used in mixtures that require a particular lightness (e.g., fine plasters or stuccoes). The presence of bassanite, an intermediate hydrated phase between anhydrite and gypsum, can be linked to an incomplete hydration process of anhydrite. The microstructural study of sulphate phases conducted via SEM–EDX has shown the simultaneous presence in many samples of calcium sulphate crystals with both the typical morphological characteristics of ground granules – a compact, crystalline structure with an average size of about 50 μm (Fig. 5b)—and as an agglomerate consisting of thin acicular crystals (10–20 μm in size) forming

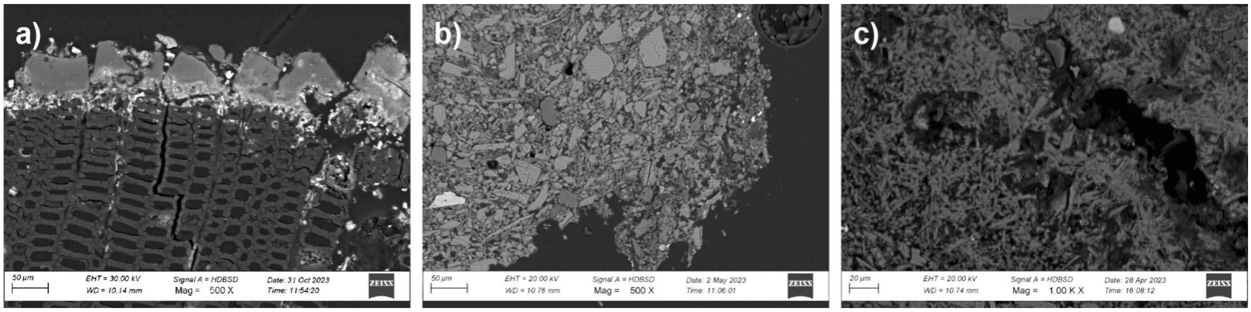

Fig. 5 Backscattered SEM–EDS images of **a** microcrystalline silica deposits on wood sample TOV_13; **b** and **c** two areas of sample TOV_17 showing different calcium sulphate micro-textures

a felt-like structure (Fig. 5c), the latter being peculiar to the hydration phenomenon of a calcium sulphate-based binder. Therefore, it can be assumed that even though theoretically, calcium sulphates in the mixture should act solely as an inert filler, in this case, they have been intentionally added, probably in the form of fine powder, to perform an additional function as an inorganic binding agent, likely supporting a more typical organic binder.

In detail, at least three types of ground layers have been recognised:

i. The first is from pure white to greyish white, depending on the number of impurities (i.e., carbon black, ochre) or carbonate fillers (calcite) included (Fig. 4a, b). Its mineralogical composition is based on calcium sulphate (gypsum and anhydrite), both used as inert and binding agents. µFTIR demonstrated the presence of an organic binder based on animal glue. Where this was not detected, weddellite was identified both through µFTIR—by identifying the typical peaks at 1621 cm^{-1} (νas C = O), 1322 cm^{-1} (νs C = O), 1136–1048 cm^{-1} (νas C-O), 882 cm^{-1} (νs C–C)—and through XRPD (in samples TOV_04, TOV_06, TOV_12, and TOV_17). This demonstrates the probable oxidative alteration of organic matter (i.e., the organic binder in the ground layer mixture) over time or possible biological mechanisms, which induced calcium oxalate development [48–51]. The layers attributable to this type tend to be the deeper and therefore older layers of the more complex stratigraphic samples (TOV_02/A, TOV_02/B, TOV_04/A, TOV_09/A) (Fig. 4).
ii. The second typology (Fig. 4c, d, e) regards yellow ground layers. The colour is due to the intentional addition of yellow ochre and carbon black particles (both with a considerable grain size) to a calcium sulphate matrix that presents similar characteristics to those described above. The layers showing this composition are listed in Table 2. In samples TOV_04 and TOV_09, these layers overlap the pre-existing ones, indicating a subsequent retouching intervention. Otherwise, samples TOV_12 and 17 are in direct contact with the wooden support, suggesting the absence of the older ground layer (*lacunae*) and the execution of pictorial integration directly on the wooden panels. It was curious and unexpected to discover that in sample TOV_10, the ground layer was applied on a polystyrene panel used as an additional element to modify the morphology of the lower part of the flat. FTIR analysis (Table 2) proved polystyrene (peaks 3600-3400, 3162-3081-3060-3025-3002, 2924-2848, 1601, 1492-1451, 1028, 758, 698 cm^{-1}) [52] and Polymethyl Methacrylate composition (peaks 3600-3400, 2924-2848, 1943-1871-1802, 1730, 1380-1328, 1276, 1197-1155, 1073, 908, 842 cm^{-1}), whereas macroscopic study of the sampling area reveals a white substrate compatible with the typical aspect of polystyrene.
iii. The last category consists of layers composed of calcium carbonate (lime) (Fig. 4b, c), an unusual feature in the panorama of paintings on wood and also in those of the Theatre. The layers with this composition are TOV_02/D and TOV_04/C (Fig. 4b, c). In sample TOV_04, this mixture occurs, stratigraphically speaking, below layer TOV_04/D, which belongs to the second type of preparation described above. This indicates that this third type belongs to an earlier intervention. The use of calcium carbonate as the principal inorganic binding agent only in these two samples leads to the assumption that retouching and/or restoration work was limited to a few flats.

The sequences of ground layers testified here present a maximum of two successive layers, sometimes with increasing grain size towards the outside instead of decreasing as required. The final layer, traditionally made of rabbit glue and applied on the preparatory strata, was matched in the C layers of TOV_02 (Fig. 4a, b) and TOV_09. SEM–EDX images clearly showed these layers to be composed of a low atomic number element (probably Carbon); furthermore, both the shape and related peaks of the FTIR spectra acquired in a sequence of layers that may also include layer C of sample TOV_02 confirmed the supposed chemical composition—3283 cm^{-1} (ν N–H), 3070, 2956–2919-2874–2851 cm^{-1} (ν C-H), 1736–1646 cm^{-1} (ν C=O), 1541 cm^{-1} (δ C-N–H), 1445–1340 cm^{-1} (δ C-H), 1243 cm^{-1} (ν C=O)—and thus correspond to the typical spectrum of animal glue [53]. In addition, as usually happens with animal glues [54–56], a bright yellow fluorescence characterises the layer when observed with RLOM in cross-section under UV light (particularly in green and blue emission).

Two exceptional cases in terms of the composition of the ground layers are identified in samples TOV_05 and TOV_06, which appear macroscopically to be fillings executed at a later date. The two impastos revealed a carbonate composition characterised by abundant traces of acrylic polymers as indicated by μFTIR analysis. It should be noted, moreover, that TOV_05 and TOV_06 do not show a true pictorial microstratigraphy: the former shows a gypsum basal layer (layer A) surmounted by a sort of thick calcium carbonate-based plastering (layer B). The second sample (TOV_06) also presents a grey-yellow, gypsum-based basal layer (layer A), followed by a thick, white, predominantly calcite layer (layer B), which is unusually filled with wood splinters. The presence of chromium oxide in layer A of sample TOV_06 also places it historically in a period certainly later than the early 1800s.

Paint layers

Pigments Table 3 summarises the most significant data from the multi-analytical study performed on the identified pigments observed in the stratigraphy of the samples. Specifications for each pigment are reported in this section.

Black Black pigment particles were identified in almost all the paint layers and numerous ground layers (Table 2). In the RLOM study, they appear in the form of opaque black particles with a mixed grain size ranging from a few microns to a maximum of approximately 100 microns even in the same sample (Fig. 6a). When analysed by μRaman these particles revealed diagnostic first-order bands in the range 1300–1600 cm^{-1} in all of the samples. In particular, two broad, overlapping bands with intensity maxima at around 1580 $cm^{-1}$and 1350 cm^{-1} (G and D bands, respectively, in Fig. 7). For a more accurate identification of the pigment, full width at half maximum (FWHM) of the D and G bands was taken into account. Indeed, Tomasini, Siracusano, and Maier in 2012 [62] report a direct connection between the increase in these values and the increase in the degree of disorder of historic pigments based on carbon. In our case, these values exceed 200 cm^{-1} and 100 cm^{-1}, respectively, placing the materials in the range of carbon-based pigments of amorphous nature. It should be noted that the peak at 961 cm^{-1} is missing, due to the PO_4^{3-} anion linked to the bone or ivory black. Moreover, the EDX investigation never detects the presence of phosphorus. The particle sizes also exclude the use of lampblack, which typically presents an extremely fine grain not detected here. This information allows us to classify this pigment as carbon-based black of the charcoal type [63].

Green Two different green pigments have been identified in the paint layer (and sometimes as occasional particles in other layers), indicating, at the very least, their presence in the artists' palettes.

The first green pigment appears in green/blue rounded semi-transparent particles under RLOM (Fig. 6b). Eastaugh et al. [63] The accurate EDX analysis performed on the green crystals in layer B of sample TOV_04 (point 2 in Fig. 6b, e) reveals a typical composition of an iron-based clay mineral with the presence of silicon and aluminium combined with magnesium, potassium, and calcium in addition to iron (Table 3). It is green earth, widely used in its various forms since antiquity, i.e. as glauconite [(K, Na)(Fe^{3+}, Al, $Mg)_2$(Si, $Al)_4O_{10}(OH)_2$] and celadonite [$K(MgFe^{3+})(Si_4O_{10})(OH)_2$] or a mixture of the two [63]. In particular, μRaman investigations confirm the identification of the pigment as a green earth and also help to make a distinction between the two more common green earths (glauconite and celadonite). Indeed, the spectra show (Fig. 7) a doublet between 170 and 200 cm^{-1}, which lacks glauconite, and the wave numbers of the two main peaks between 250 and 400 cm^{-1} are higher (i.e., around 270 and 394–400 cm^{-1}). Furthermore, in the region between 550 and 600 cm^{-1}, the most intense peak is at around 550 cm^{-1} and not at 590 cm^{-1} as required by glauconite [60]. All these Raman features are typically for celadonite (Fig. 7), suggesting the use of the excellent-quality *Terra verde di Verona* pigment, which was identified by previous studies as green earth precisely based on celadonite [63].

The second green pigment only appears in layer A of sample TOV_06 and layer C of sample TOV_17, showing rounded green particles under RLOM. The μRaman spectrum (Fig. 7), acquired in correspondence with green/yellow particles, shows the diagnostic peaks of the mineral eskolaite (Cr_2O_3), which identify the pigment as chromium oxide, the synthetic form of the mineral (Table 3).

Table 3 Most representative results for pigments

Pigment	Colour	Sample	EDS	Raman (cm^{-1})	XRPD	First use	References
Carbon-based black	Black	TOV_02; TOV_03; TOV_04; TOV_05; TOV_06; TOV_09; TOV_10; TOV_11; TOV_12; TOV_15; TOV_17		1580, 1335 (TOV_03/B)		Prehistory	[57]
Red ochre	Red	TOV_02; TOV_03; TOV_04; TOV_05; TOV_09; TOV_10; TOV_12; TOV_17	Fe, Ca, Si, S, Mg, Al (TOV_02/E)	610, 495, 413, 296, 246, 228, 113 (TOV_02/D)		Prehistory	[58]
Yellow ochre	Yellow	TOV_02; TOV_03; TOV_04; TOV_05; TOV_06; TOV_09; TOV_10; TOV_11; TOV_12; TOV_15; TOV_17	Fe, Si, Zr, Ca, Al, Mg, S (TOV_06/A)	550, 446, 393, 294, 247, 206 (TOV_02/D)	Goethite (TOV-17/B)	Prehistory	[58]
Dolomite	White	TOV_09; TOV_17		1099, 298, 178		Prehistory	[59]
Green earth	Green	TOV_02; TOV_04; TOV_10	Si, Fe, Mg, K, Al, Ca (TOV_04/B)	702, 546, 395, 278, 216, 176 (TOV_04/B)		Antiquity	[60]
Indigo	Blue	TOV_09		1575, 1484, 1463, 1366, 1313, 1249, 1227, 759, 676, 600, 546, 277, 266, 253, 135, 97 (TOV_09/G)		Antiquity	[61]
Lead/Sulphur-based pigment	White	TOV_09	Pb, S, Cl, Fe, Ti (TOV_09/B)				
Barium white	White	TOV_02; TOV_03; TOV_04; TOV_05; TOV_06; TOV_09; TOV_10; TOV_11; TOV_12; TOV_15; TOV_17	Ba, S, Ca, Si (TOV_17/C)	986, 645, 615, 451, 233, 75 (TOV_15/C)	Barite (TOV_17/C)	1800s	[58]
Chromium oxide	Green-yellow	TOV_06; TOV_17		612, 555, 351, 297 (TOV_06/A)		early 1800s	[58]
Titanium white	White	TOV_02; TOV_03; TOV_04; TOV_05; TOV_06; TOV_09; TOV_10; TOV_11; TOV_12; TOV_15; TOV_17	Ti, Si, Ca, S, Al, Na, K, Mg (TOV_11/C)	rutile—610, 446, 244–231, 141 (TOV_11/C) anatase—637, 515, 393, 142 (TOV_12/C)	Titanium oxide (TOV_05/A)	Confirmed after 1930s (first produced in 1916)	[61]

In brackets, the sample/layer to which the data refers. References used for spectral interpretation are also reported

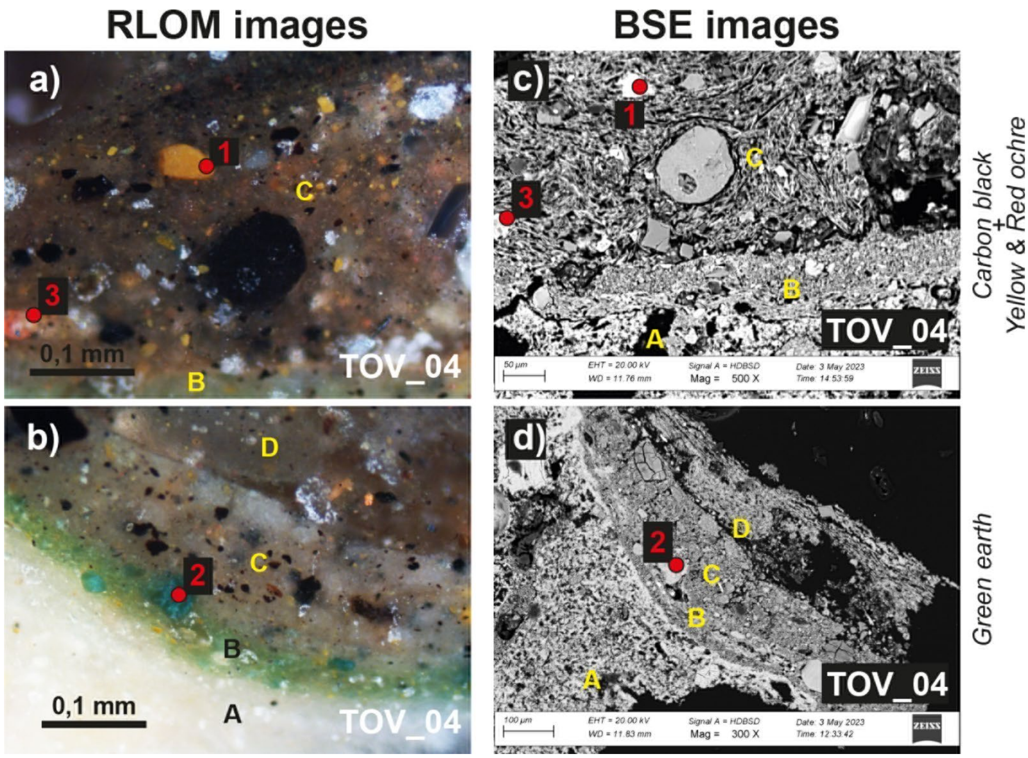

Fig. 6 Reflected-light photomicrographs of a cross-section of the sample (**a**, **b**); backscattered SEM–EDS images of the same samples (**c**, **d**)

Typically, the pigment is opaque, olive-green, generally known as chrome oxide or Casali's green. It was introduced in the early nineteenth century and first detected in Turner's 1812 paintings [64].

Red The red on the wooden flats can be linked to a single pigment. It occurs under RLOM in deep red particles, often agglomerated and associated with very fine-grained mineral particles (clay minerals). EDX analysis reveals high iron contents (Fig. 6a, point 3), which can be associated with the presence of the mineral hematite (Fe_2O_3) and lower percentages of silicon, magnesium, and/or aluminium that can be linked to the clay portion. Calcium and sulphur are also often present, possibly due to background noise from the gypsum component surrounding the particles (Table 3). The pinpointed μRaman investigation identifies hematite, which undoubtedly appears with the two very strong intensity bands at around 220 and 290 cm^{-1} and the medium intensity band at about 400 cm^{-1} (Table 3, Fig. 7). The coexistence of hematite and clay minerals enables the pigment to be defined as red ochre.

It is well known that ochres have been in constant use as pigments since prehistoric times [63]. Moreover, their provenance is extremely vast and very difficult to discern due to the extensive distribution of deposits from which this pigment can be obtained [65].

Yellow As in the case of red, the analyses discovered only one type of yellow pigment. It occurs under RLOM in opaque yellow particles often agglomerated and associated with very fine-grained mineral particles (clay minerals), having grain size from a few microns to a few tens of microns, depending on the sample and layer (Figs. 4a,d and 5a). Also, in this case, the analyses carried out by EDX on yellow particles (point 1 in Fig. 6a, d) revealed the abundant presence of iron – most probably referred to goethite [α-$Fe^{3+}O(OH)$] or other forms of iron hydroxide and oxides (i.e., limonite, here intended as unidentified massive hydroxides and oxides of iron, with no visible crystals) – together with the presence of silicon, aluminium, magnesium, attributable to the clay portion, with traces of zircon (Table 3). Once again, sulphur and calcium are more likely correlated with the gypseous components surrounding the analysed particles. The μRaman investigation revealed the diagnostic peaks of goethite. Therefore, the fundamental peaks are intense at about 390 cm^{-1} and the medium intensity at about 290 cm^{-1} (Table 3). The mixture of clay minerals with iron hydroxides and oxides, including goethite, allows this pigment to be defined as yellow ochre.

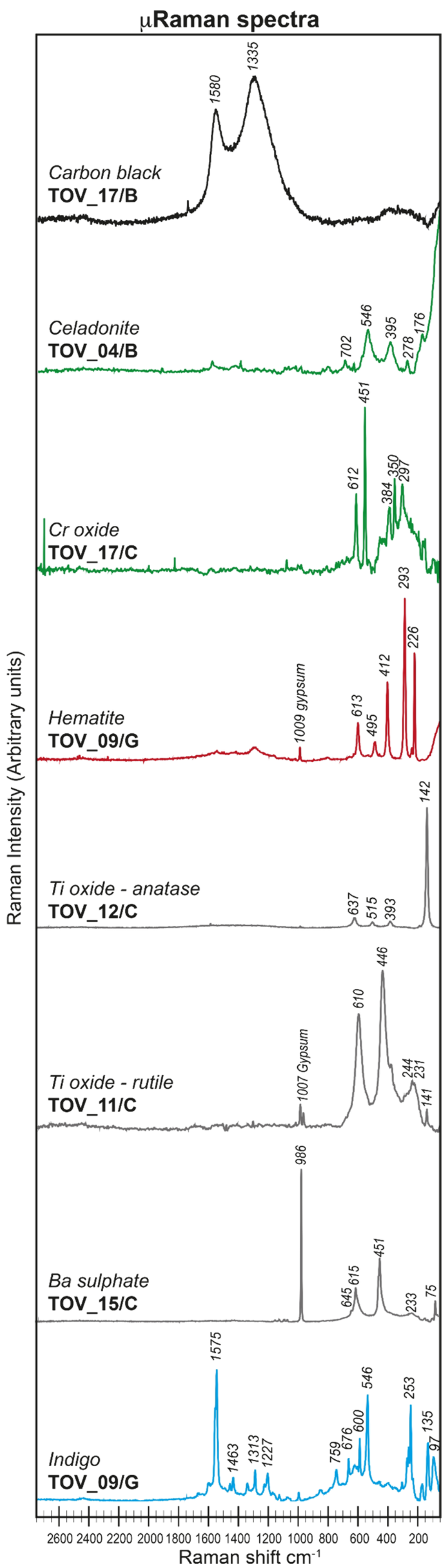

Fig. 7 Pigments. Raman spectra of the most significant pigments

Regarding this pigment's historical use and origin, what has already been said about red ochre also applies to yellow ochre [65].

White The white pigments identified are by far the most numerous, and most of these are modern (i.e., after the second half of the nineteenth century).

μRaman investigation detected diagnostic peaks at 1099, 298, and 178 cm^{-1} in two paint layers, TOV_09/E and TOV_17/B, and in the ground layer TOV_06/B, which identifies the mineral dolomite [$CaMg(CO_3)_2$]. The XRPD analysis of sample TOV_06 confirmed this attribution. However, only in layer TOV_09/E can its use be attributed as a pigment, while in the other two cases, it is a generic carbonate filler.

The use of dolomite as a pigment is certainly known from Hellenistic and Roman times, although it was not widespread [63].

An unusual white pigment based on lead and sulphur was detected through EDX investigations only in TOV_09. The elemental mapping reported in Fig. 8 showed the superimposed distribution of sulphur and lead mainly concentrated in layer B (red arrow in Fig. 8) and traces in layers E and H. In the literature, lead sulphate is the only pigment that seems to fit this composition [63]. However, attributing these particles to this pigment seems highly improbable in the context of the *Teatro Olimpico*. Moreover, the historical-temporal location of lead sulphate is not clearly defined. Indeed, it only vaguely figures among the pigments used for artistic purposes. It is, for example, identified by Winter [66] in thirteenth–sixteenth -century Chinese paintings. At the same time, Harley [67] suggests its use in watercolours made in Great Britain in the late 18th and early nineteenth century, when it appears to have been marketed under the name "Flemish white" by painters who followed instructions dating back to the late eighteenth century for its preparation. Lead sulphate still appears in many modern industrially produced pigments.

The analyses revealed two additional types of white pigments. The RLOM study did not enable the two pigments to be differentiated but only detected the presence of a very thin superficial layer (a few tens of micrometres thick) appearing as a homogeneous white-to-yellowish hue (Table 2). On the other hand, SEM–EDX showed titanium-rich particles, occasionally accompanied by lower amounts of other elements (Si, Ca, S, Al, Na, K, Mg) due to background noise from surrounding fillers. These particles were uniformly distributed in the paint finish with a very fine grain size (Fig. 8b). These were paired with barium-rich particles, which were larger in size (up to a few tens of micrometres) and less widespread in the paint layers; they exhibited a chemical

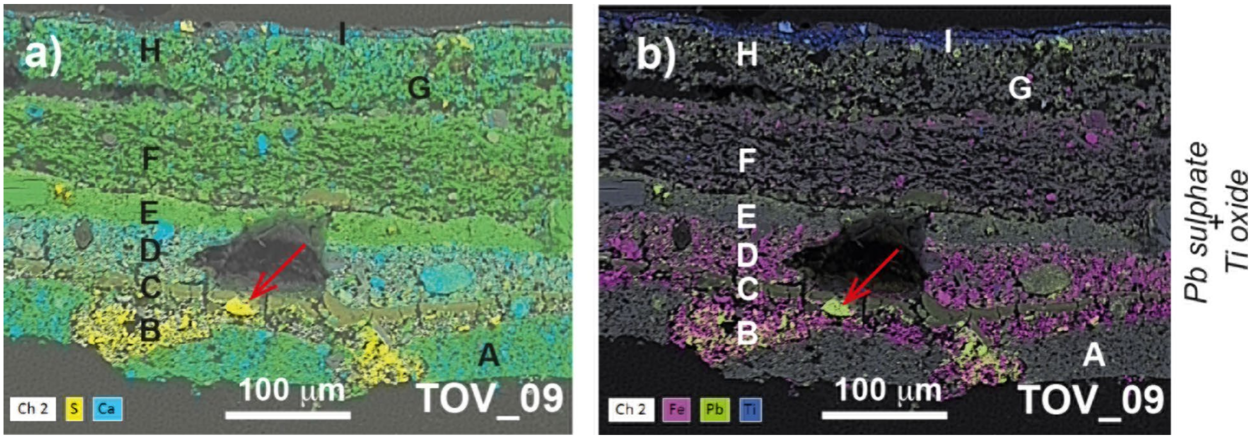

Fig. 8 Elemental EDX maps of sample TOV_09, in false colours

composition comprising barium and sulphur, with traces of calcium and silicon likely due to contamination from surrounding materials (Table 3). Both pigments were found together in extremely thin paint layers covering all the samples analysed, as shown by the SEM–EDX elemental map (Fig. 8). However, recognising dispersed barium sulphate particles using mapping mode proved challenging due to the unavoidable overlap of energy peaks crucial for the recognition of Ti and Ba (i.e., Kα at 4,5 keV and Kβ at 4,9 keV for titanium and Lα at 4,5 keV and Lβ at 4,8 keV for barium). Nevertheless, point investigation obviated this factor using other energy peaks, and confirmed the simultaneous presence of barium sulphate and titanium dioxide in the superficial layers of all the samples. Furthermore, XRPD recognised barite and a generic titanium oxide (Table 3). And µRaman analysis revealed diagnostic peaks for barium sulphate (Table 3, Fig. 7) and attested two different crystalline forms of titanium dioxide (TiO_2). Diagnostic peaks of the rutile mineral form were found in the TOV_11/C layers, while those of the anatase form were found in the TOV_12/C and TOV_17/C layers, which would seem to indicate the use of two different titanium pigments (Table 3, Fig. 7). Various observations led us to exclude the possibility of a natural origin for TiO_2. Firstly, its colour differs from that of the natural mineral rutile, which never exhibits the bright white hue characteristic of synthetic titanium dioxide. Secondly, no accessory minerals potentially originating from natural deposits were identified. Instead, the coexistence of rutile and anatase could be linked to various methodologies of synthetic pigment production. Historically, the chloride process, involving the vapour-phase oxidation of titanium tetrahalides, utilized mineral rutile as its starting raw material. This method was introduced in Germany in the 1950s [63]. Thus, the white pigments are titanium white (titanium oxide, TiO_2) and barium white or *bianco fisso* (barium sulphate, $BaSO_4$), historically used in various mixtures.

It is worth mentioning that titanium white, first produced in 1916, did not establish its presence as a pigment until after the First World War, and it was only unanimously accepted and recorded in art manuals in the 1930s [63]. In comparison, barium sulphate was used as a white pigment from the beginning of the nineteenth century [63].

Blue Only one blue pigment was detected. Under RLOM, it appears as blue angular particles with a vitreous appearance. Although characterised by an intense blue hue, it was found in two layers, G and H, of sample TOV_09, appearing macroscopically brown/grey and green, respectively. µRaman investigation identified it unequivocally in both sample layers, and the spectra collected showed all peaks referred to the natural dye indigo [61] (Table 3, Fig. 7).

Indigo was known and used in antiquity. It owes its blue hue to a natural dye derived from the leaves of various species of *Indigofera*. The procedures and materials used to prepare stable lacquers are numerous. For example, the clay mineral palygorskite was used to produce the famous Maya blue [63]. Its presence in superficial paint layers characterized by the presence of acrylic resin suggests a synthetic and recent origin. Additionally, certain spectral features recognized in the µRaman spectrum, such as the resolution of one of the characteristic peaks between 1582 and 1571 cm^{-1}, would confirm this hypothesis [68].

Comparing the palette detected on the *Teatro Olimpico* flats, excluding the pigments found in the more recent layers, with that recognized in paintings from the same historical period or from the Renaissance, it emerges clearly how the pigments here are very simple and basic (ochre, earth, carbon black). The pigments found elsewhere are generally more refined and precious. There is widespread mention of vermilion, madder lake, lapis lazuli, verdigris, and azurite [69, 70], and this is also the case in nearby Venice [71]. Pigments such as azurite or cinnabar can already be found in some productions of decorative wooden ceiling panels from the previous century (fifteenth century), such as those studied in Cremona (northern Italy), which recall the most widespread technologies in northern Europe [73].

Organic binders and retouching The complexity of the case study is also reflected in the definition of the original binders.

However, traditional organic materials were identified as present in the original painting in only a few cases. Indeed, in layer E of sample TOV_02, μFTIR revealed the presence of the characteristic peaks of a binder of proteinaceous nature (3282 cm^{-1} due to ν N–H, 3067 cm^{-1}; 2956–2919-2873–2850 linked to ν C–H, 1731; 1646 cm^{-1} attributed to ν C=O, 1541 δ C–N–H; 1444–1399 cm^{-1} corresponding to δ C-H, and 1242 cm^{-1} linked to ν C=O), whereas in sample TOV_03 the spectrum of the paint layer showed the presence of Arabic gum (3346 cm^{-1} due to ν O–H; 2900 cm^{-1} linked to ν C–H; 1639 cm^{-1} attributed to δ O–H, and 1427–1316 cm^{-1} corresponding to νas C–H). Arabic gum could possibly have been used as a medium for tempera and watercolour. It may also have been applied as an adhesive in the assembly of wood elements during restoration. Ground layers of samples TOV_04, TOV_05, TOV_06, TOV_12 and TOV_17 showed the presence of weddellite correlated to the alteration of the organic substance as described in "Ground layers" section.

In contrast, all the samples have a modern acrylic component in the superficial layers (2990–2870 cm^{-1} ν C-H; 1730 cm^{-1} ν C=O; 1475–1440 cm^{-1} δas C-H; 1235 cm^{-1} ν C=O; 1145 cm^{-1} νas C–C(=O)-O, 1026 cm^{-1} ν O-C–C). The multi-analytical study revealed a very thin external layer (between 10 and 20 μm thick), generally white, based on acrylic resin rich in titanium and barium white on all the samples. This chemical composition is clearly of modern date since the two white pigments only became widespread in more recent times, as already mentioned in "White" section. Furthermore, it was only in the second half of the twentieth century that the advent of plastics led to the use of acrylic-type paints in fine art as well. It can therefore be assumed that the application of this thin film dates from the relocation of the scenery after World War II or later. A good example of this reasoning is shown in Fig. 4f, g, h, in which the μFTIR map of TOV_04 proved the chemical composition of the acrylic binder in layer TOV_04/C just above the green paint layer TOV_04/B. This factor dates the retouching operation to at least the second half of the twentieth century. This layer, which is macroscopically almost transparent due to its thinness, may have been applied in order to enhance/revive the chromatic effect and homogenise the macroscopic appearance of the reconstructed set of flats. However, the characteristic peaks were also detected in the paint layers below all the samples. Since μFTIR maps did not identify continuous layers based on acrylic nature in the lower strata but only sporadic traces, it may be supposed that acrylic paint was used for localised retouching or that acrylic matter intended only for the paint surface in fact penetrated the porosity of the pictorial stratigraphy [72].

Based on the microstratigraphic study, although the paint layers just beyond the first type of ground layer in samples TOV_02, 04 and 09 are not precisely datable, they can nevertheless be considered the earliest of the pictorial finishes. There is a change of colour from the deeper layers of the stratigraphy to the colour of the most superficial layer currently perceptible on the flat. Indeed, there is a change from pale yellow (layer D) to yellowish brown (layer G) for sample TOV_02 (Fig. 4a), from green (layer B) to orange (layer F) for sample TOV_04 and from red (layer B) to green/grey (layer G/H) for sample TOV_09.

Samples TOV_03, TOV_11 and TOV_15 present a very simple and unique microstratigraphy compared to the others. They show a white sulphate preparation layer from the inside to the outside, with a few dispersed red and yellow ochre particles on top of the wooden support. Laid directly on this is a very thin layer (layer C) containing the usual titanium white and coarser particles of barium white dispersed in a binder of an acrylic nature.

Three-dimensional model data visualisation and cataloguing for preservation

Through a targeted analysis of front 3A of flat 3, querying an element within the HBIM model yields the information detailed in Table 4.

Information about the transformations of the fronts and the images, whether historical or current, has been linked to external folders. The HBIM thus offers a further possibility for managing the model: the dynamic link, which can also be updated like all the other information above, leads to folders whose content can be expanded as the search goes on. In the case of this research, it was possible, for example, to link historical post-war black-and-white photographs and shots taken during the surveys, relating the photographic data by individual front, facilitating the interpolation of information and the identification of differences. This operation made it possible to investigate the limits in the pictorial films and

Table 4 Example of data obtainable from the HBIM system interrogation

Entity data	
Dating	1585
Author	Vincenzo Scamozzi
Transformations	External link: intervention history > history of interventions on flats
Materials	Silver Fir (Abies Alba) and Spruce (Picea Abies)
Construction characteristics	Wooden panel assembly
State of conservation	Fair characterized by slight degradation [73]
Critical issues	Abrasions, discolouration, cracks, graffiti, lacunae in the paint film, lacunae in the ground layer, missing parts, blistering, xylophagous attack, coherent deposit, incoherent deposit [74]
Investigations carried out	Thermography, micro-sampling, ultrasonic tests, microclimate monitoring
Investigations to be carried out	microclimate monitoring
Historical iconography	External link: documentation > historical iconography
Photographs	External link: documentation > photographic documentation
Critical issues	Abrasions, discolouration, cracks, graffiti, lacunae in the paint film, lacunae in the ground layer, missing parts, blistering, xylophagous attack, coherent deposit, incoherent deposit
Operations to be undertaken	Restoration of the pictorial finishes

decorations between original portions and 20th-century repainting, a completely new element never associated before. Figure 1 shows the relationship with the same portion of the scenery as photographed in 1944, before they were dismantled, and the same viewpoint repurposed in 2023, making it possible to compare the state of conservation of the surfaces.

Through the critical evaluation of previous analyses and the observation of historical images, it emerged that front 3A had not been subjected to sampling. For this reason, the research team decided to focus the investigation on the less studied areas, as shown in Table 1. Table 4, on the other hand, summarizes the information shown by the HBIM when an element has been selected within the model. The information related to Table 1 are graphically proposed in the three columns of the Fig. 3.

It is also possible to have an indicative quantification of the state of conservation of the selected element with a five-grade scale—good, fairly good, fair, poor, very poor—associated with a degradation assessment scale—very slight, slight, moderate, severe, very severe [73].

The laboratory investigations revealed that the pictorial cycle of the scenery that belonged to Scamozzi's era might have been different, both from a chromatic and compositional point of view, with particular reference to the replaced portions, the additions, and the different materials used to repaint the wooden supports. The results reported here testify in several cases to the chromatic modification undergone by the flats (samples TOV_2, TOV_4, and TOV_9), probably in response to changes in taste or, otherwise, to highlight certain architectural elements over others (a paper is currently being prepared, to explain in greater detail the correlation between the mapping of the historical paintings as seen in the 1944 photos and the micostratigraphies found in the pictorial finishes of the *Teatro Olimpico* flats). Figure 1 shows the relationship between the appearance of the wooden flats before they were dismantled and how they appear today.

This information can be visualised by three-dimensional axonometric exploded view processing, as shown in Fig. 9. The three-dimensional visualisation allows a detailed overall view from a single viewpoint, guaranteeing, on the one hand, the placement of the individual sample in the general layout of the facade, and on the other hand, an accurate understanding of the laboratory analyses performed as well as the associated results.

In particular, through the photogrammetric survey, it was possible to obtain an orthophoto of the flat—in this case the 3A front—which was digitally drawn. Samples and details of the results of the analyses carried out in the current and previous investigations were then inserted. The subsequent analytical determination of their composition showed which parts are original and which were repainted. Figure 9 shows an example of a system interrogation using samples TOV_4, TOV_9 and TOV_10. The upper part of the image displays the entire 3A front, from which the three portions related to the samples examined were exploded. The lower part of the image, on the other hand, shows all the details related to the laboratory investigations performed on the samples taken from the flat, with a three-dimensional visualization of the thin section of the sample that can help in understanding the complex layering of the element. The image highlights

Fig. 9 Isometric view of the 3A front of Scamozzi's scenery for the *Teatro Olimpico* in Vicenza. The upper part of the figure shows Flat 3A broken down into its architectural components; the lower part shows the location of samples taken from three different points on the flat, the analyses to which each was subjected and the conclusions drawn with respect to the stratification of the paint and ground layers

the three-dimensional modelling of the individual sample and makes it possible to visualise both the methods of investigation applied and the stratigraphy of the paint films; each layer has been coded with an identifying letter and linked to a legend, which provides details of its composition as detailed in "Paint microstratigraphy" section. The model, of which Fig. 9 presents a simple example of data extraction, can thus generate an infinite number of search possibilities. Through the selection of a single object (a portion of a wooden flat, a single architectural element, etc.) it is possible to obtain detailed information concerning it. This makes it possible to systematize historical data and results from laboratory analyses, starting from the overall view of the architectural element being interrogated (scene, column, portion) and arriving at the single sample taken. The three-dimensional model data visualisation thus offers an agile synthesis between the overall vision of the selected architectural object backed by studies typically conducted on it by art historians, critics and architects, and a detailed view, at a smaller scale, that characterises the typical contributions of applied mineralogists and petrographers, chemists and restorers working in heritage science. This holistic, multiscale view is one of the innovative results of using HBIM as a tool for investigation and design in the restoration of material and tangible cultural heritage.

Conclusions

The methodological approach adopted for research on the *Teatro Olimpico* in Vicenza proved the potential of an interdisciplinary study to enhance and maintain a site of significant cultural and historical interest. On one hand, the diagnostic enabled significant observations to be made on the materials and technologies used for the painting of the wooden scenery, identifying the materials applied and distinguishing the original ones from those related to modern restorations of the panels, an important advance evidenced here for the first time. The investigations confirmed complex and varied sequences regarding the microstratigraphic sequence and painting technology, indicating that the wooden perspective flats had undergone numerous retouching and restoration interventions. The laboratory data revealed a rather basic pigment palette, especially concerning the hypothetically older layers (i.e., ochres, green earth and carbon blacks). Indigo is the only exception to this uniformity. The pervasive presence of acrylic polymers, especially in the surface layers, as well as the ubiquitous use of titanium oxide and barium sulphate, are evidence of further modern reworking.

The use of a Heritage Building Information Modelling (HBIM) system facilitated the digitization of all the acquired documents and data related to the *Teatro Olimpico* in Vicenza, and contributed significantly to identifying and guiding the selection of sampling points through meticulous evaluation of historical information. The analyses performed acquire a peculiar importance by cataloguing all the research carried out, both completed and in progress, for a timely analysis of the historical relevance of the traces of original and modern paint that can guide the conservation process in the operational choices related to them. In addition, the model enables a programme to be developed, detailing new insights and investigations to be carried out to increase the level of knowledge. By keeping the model updated with the restoration work carried out, it will be possible to monitor the response of the materials to interventions on the wooden scenery as a function of the microclimatic indoor conditions of the *Teatro Olimpico*, to set up monitoring programmes and to plan scheduled conservation. An added value of the methodology described is the high potential for sharing which will avoid future data dispersion (as is the case of the unpublished data on the repainted sections of the scenery) as all those involved in the restoration process will be able to update the information in the digital model as studies and interventions continue. Finally, the HBIM system allows consolidation of all the acquired building data into a unified digital model facilitating the creation of connections and correlations between the information collected.

Acknowledgements

We would like to thank all the institutions involved for their collaboration, including the Soprintendenza of Verona, which engaged Università Iuav to carry out this research, the Municipality of Vicenza and the *Teatro Olimpico*, which allowed the surveys to be carried out and actively collaborated in assisting the personnel involved. The authors are also grateful to the Laboratorio di Fotogrammetria (Photogrammetry Laboratory) of the *Università* Iuav *di Venezia* for its support in processing the data obtained from the topographic and laser scanning survey.

Author contributions

Conceptualization, F.A., and E.S.; Methodology, F.A., R.P., E.S. and E.T.; Validation, F.A., R.P., E.S. and E.T.; Formal Analysis, R.P., E.T., E.S. and M.T.; Investigation, R.P., E.T., F.A. E.S. and M.T.; Writing – Original Draft Preparation, R.P., E.S. and M.T.; Writing – Review & Editing, F.A., R.P., E.S., E.T., and M.T.; Visualization, R.P., E.S. and M.T.; Supervision, F.A., and E.S.; Project Administration, E.S.; Funding Acquisition, E.S. All authors have read and agreed to the published version of the manuscript.

Funding

The current research project entitled "Metodi e analisi di conoscenza preliminare al progetto di restauro del *Teatro Olimpico* di Vicenza" is part of a framework of collaboration, started in 2019, between the Soprintendenza Archeologia, Belle Arti e Paesaggio for the provinces of Verona, Rovigo and Vicenza and the Università Iuav di Venezia that has included the stipulation of several agreements, under the scientific coordination of Professor Emanuela Sorbo. In particular, the current research project is included within the Framework Agreement stipulated in 2021 between the Soprintendenza Archeologia, Belle Arti e Paesaggio for the provinces of Verona, Rovigo and Vicenza and the MATESCA cluster of the Università Iuav di Venezia financed with funds from the Ministry of Culture, allocated for the conservation project for the *Teatro Olimpico* in Vicenza.

Availability of data and materials

The datasets generated and/or analysed during the current study are not publicly available due to the co-ownership of the data with the Italian Ministry of Culture but are available from the corresponding author on reasonable request.

Declarations

Competing interests

The authors declare that they have no competing interests.

Received: 15 January 2024 Accepted: 30 May 2024
Published online: 18 June 2024

References

1. Forlati F. Restoration of war-damaged buildings - province of Vicenza (in Italian: Restauro di edifici danneggiati dalla guerra - prov. di Vicenza). Bollettino Dell'Arte II. 1952;I:266–76.
2. Zurli F. Restorations in progress in Palladio's buildings (in Italian: Restauri in atto nelle fabbriche palladiane). Bollettino del CISA Andrea Palladio XX. 1979;I:302–3.
3. Magagnato L. The Teatro Olimpico (in Italian: Il Teatro Olimpico). Milan: Electa; 1992.
4. Cafà V. Interventions on the Teatro Olimpico in Vicenza (1584–1585), in: Vicenzo Scamozzi 1548-1616- Exhibition catalogue (in Italian: Interventi sul Teatro Olimpico a Vicenza (1584–1585), in: Vicenzo Scamozzi 1548-1616-Catalogo della mostra), Vicenza, Museo Palladio, 7 September 2003-11 January 2004, Marsilio, Venezia; 2003, p. 250–259.
5. Carunchio T. Investigations of the teatro olimpico in Vicenza (in Italian: Indagini conoscitive sul teatro Olimpico di Vicenza). In: Magagnato L, Puppi L, editors. The teatro olimpico (in Italian: Il Teatro Olimpico). Milano: Electa; 1992, p. 129–40.
6. Danzi E. The Teatro Olimpico: some constructive transformations observed with the support of stratigraphic analysis (in Italian: Il Teatro Olimpico: alcune trasformazioni costruttive osservate con l'ausilio dell'analisi stratigrafica). In: Piana M, Soragni U, editors. Palladio: materials techniques restoration: in honour of Renato Cevese (in Italian: Palladio: Materiali Tecniche Restauri: in onore di Renato Cevese). Venice: Marsilio; 2011, p. 12–22.
7. Piana M, Soragni U, editors. Palladio: materials techniques restoration: in honour of Renato Cevese (in Italian: Palladio: materiali, tecniche, restauri in onore di Renato Cevese). Marsilio: Venice; 2011.
8. Gomes H, Rosina P, Holakooei P, Solomon T, Vaccaro C. Identification of pigments used in rock art paintings in Gode Roriso-Ethiopia using Micro-Raman spectroscopy. J Archaeol Sci. 2013;40:4073–82. https://doi.org/10.1016/j.jas.2013.04.017.
9. Durkin-Meisterernst D, Friedrich M, Hahn O, Helman-Wazny A, Nöller R, Raschmann SC. Scientific methods for philological scholarship: pigment and paper analyses in the field of manuscriptology. J Cult Herit. 2016;17:7–13. https://doi.org/10.1016/j.culher.2015.06.004.
10. Pagano S, Germinario C, Alberghina MF, Covolan M, Mercurio M, Musmeci D, Piovesan R, Santoriello A, Schiavone S, Grifa C. Multilayer technology of decorated plasters from the domus of Marcus Vipsanus Primigenius at Abellinum (Campania Region, Southern Italy): an analytical approach. Minerals. 2022. https://doi.org/10.3390/min12121487.
11. Holakooei P, Karimy AH, Piovesan R, Hosseinzadeh J, Javeri M, Antonelli F, Maritan L. Make up in the grave: scientific analysis of contents of the so-called kohl pots at the archaeological site of Estark-Joshaqan, central Iranian plateau. Archaeol Anthropol Sci. 2022. https://doi.org/10.1007/s12520-022-01511-8.
12. ICOMOS. The Burra Charter: the Australia ICOMOS charter for places of cultural significance 2013. 2013. https://australia.icomos.org/wp-content/uploads/The-Burra-Charter-2013-Adopted-31.10.2013.pdf. Accessed 2 Oct 2023.
13. van der Werf ID, Gnisci R, Marano D, De Benedetto GE, Laviano R, Pellerano D, Vona F, Pellegrino F, Andriani E, Catalano IM, Pellerano AF, Sabbatini L. San Francesco d'Assisi (Apulia, South Italy): study of a manipulated 13th century panel painting by complementary diagnostic techniques. J Cult Herit. 2008;9:162–71. https://doi.org/10.1016/j.culher.2007.10.003.
14. Pięta E, Proniewicz E, Szmelter-Fausek B, Olszewska-wietlik J, Proniewicz LM. Micro-Raman spectroscopy analysis of the 17th century panel painting "Servilius Appius" by Isaac van den Blocke. J Raman Spectrosc. 2014;45:1019–25. https://doi.org/10.1002/jrs.4489.
15. Pellerito C, Di Marco AE, Di Natale MC, Pignataro B, Scopelliti M, Sebastianelli M. Scientific studies for the restoration of a wood painting of the Galleria Interdisciplinare Regionale della Sicilia-Palazzo Mirto di Palermo. Microchem J. 2016;124:682–92. https://doi.org/10.1016/j.microc.2015.10.033.
16. Stanzani E, Bersani D, Lottici PP, Colomban P. Analysis of artist's palette on a 16th century wood panel painting by portable and laboratory Raman instruments. Vib Spectrosc. 2016;85:62–70. https://doi.org/10.1016/j.vibspec.2016.03.027.
17. Lambert FEM, Ornik J, Staats NA, Jäckel A, Hernandez-Cardoso GG, Taiber J, Stübling EM, Rudolph B, Mack O, Portsteffen H, Castro-Camus E, Koch M. Layer separation mapping and consolidation evaluation of a fifteenth century panel painting using terahertz time-domain imaging. Sci Rep. 2022. https://doi.org/10.1038/s41598-022-25013-8.
18. Sfarra S, Ibarra-Castanedo C, Ambrosini D, Paoletti D, Bendada A, Maldague X. Integrated approach between pulsed thermography, near-infrared reflectography and sandwich holography for wooden panel paintings advanced monitoring. Russ J Nondestr Test. 2011;47:284–93. https://doi.org/10.1134/S1061830911040097.
19. García-Bucio MA, Casanova-González E, Ruvalcaba-Sil JL, Arroyo-Lemus E, Mitrani-Viggiano A. Spectroscopic characterization of sixteenth century panel painting references using Raman, surface-enhanced Raman spectroscopy and helium-Raman system for in situ analysis of Ibero-American Colonial paintings. Philos Trans Royal Soc Math Phys Eng Sci. 2016. https://doi.org/10.1098/rsta.2016.0051.
20. Dandolo CLK, Cosentino A, Jepsen PU. Inspection of panel paintings beneath gilded finishes using terahertz time-domain imaging. Stud Conserv. 2015;60:S159–66. https://doi.org/10.1179/0039363015Z.000000000220.
21. Ibarra-Castanedo C, Sfarra S, Ambrosini D, Paoletti D, Bendada A, Maldague X. Diagnostics of panel paintings using holographic interferometry and pulsed thermography. Quant Infrared Thermogr J. 2010;7:85–114. https://doi.org/10.3166/qirt.7.85-114.
22. Groves RM, Pradarutti B, Kouloumpi E, Osten W, Notni G. 2D and 3D non-destructive evaluation of a wooden panel painting using shearography and terahertz imaging. NDT and E Int. 2009;42:543–9. https://doi.org/10.1016/j.ndteint.2009.04.002.
23. Dooley KA, Conover DM, Glinsman LD, Delaney JK. Complementary standoff chemical imaging to map and identify artist materials in an early Italian renaissance panel painting. Angew Chem. 2014;126:13995–9. https://doi.org/10.1002/ange.201407893.
24. Picollo M, Fukunaga K, Labaune J. Obtaining noninvasive stratigraphic details of panel paintings using terahertz time domain spectroscopy imaging system. J Cult Herit. 2015;16:73–80. https://doi.org/10.1016/j.culher.2014.01.006.
25. Balletti C, Guerra F, Scocca V, Gottardi C. 3D integrated methodologies for the documentation and the virtual reconstruction of an archaeological site, International Archives of the Photogrammetry, Remote Sensing and Spatial Information Sciences - 3D Virtual Reconstruction and Visualization of Complex Architectures, 25-27 February 2015, Avila, Spain XL-5/W4. 2015; 215–222. https://doi.org/10.5194/isprsarchives-XL-5-W4-215-2015.
26. Chiabrando F, Sammartano G, Spanò A. Historical buildings models and their handling via 3d survey: from points clouds to user-oriented HBIM, in: The International Archives of the Photogrammetry, Remote Sensing and Spatial Information Sciences, Volume XLI-B5, 2016 XXIII ISPRS Congress, 12–19 July 2016, Prague, Czech Republic, International Society for Photogrammetry and Remote Sensing. 2016; 633–640. https://doi.org/10.5194/isprsarchives-XLI-B5-633-2016.
27. Palluchini R. Vincenzo Scamozzi's profile (in Italian: Profilo di Vincenzo Scamozzi). Bollettino Del CISA Andrea Palladio II. 1961;I:89–101.
28. Avagnina ME. The Teatro Olimpico (in Italian: Il Teatro Olimpico). 3rd ed. Venezia: Marsilio; 2011.
29. Barbieri F, Beltramini G. Vicenzo Scamozzi 1548-1616, Venezia, 2003.
30. Puppi L. Brief history of the Teatro Olimpico (in Italian: Breve storia del Teatro Olimpico). Vicenza: Neri Pozza; 1973.
31. Nogara G. Chronology of performances in the Teatro Olimpico in Vicenza from 1585 to 1970 (in Italian: Cronache degli spettacoli nel teatro Olimpico di Vicenza dal 1585 al 1970), Accademia Olimpica; 1972.
32. Volk R, Stengel J, Schultmann F. Building Information Modeling (BIM) for existing buildings—literature review and future needs. Autom Constr. 2014;38:109–27. https://doi.org/10.1016/j.autcon.2013.10.023.
33. Brumana R, Della Torre S, Previtali M, Barazzetti L, Cantini L, Oreni D, Banfi F. Generative HBIM modelling to embody complexity (LOD, LOG, LOA, LOI): surveying, preservation, site intervention—the Basilica di Collemaggio (L'Aquila). Appl Geomat. 2018;10:545–67. https://doi.org/10.1007/s12518-018-0233-3.

34. Guerra G, Balletti C, Sorbo E, Spironelli G. The construction of an informative model. Limits and opportunities of Historical/Heritage Building Information Modeling (in Italian: La costruzione di un modello informativo. Limiti e opportunità dell'Historical/Heritage Building Information Modeling). In: Sorbo E, editor. Ruin. Unfinished church of San Michele Arcangelo in Brendola. Tools for Knowledge, Valorisation and Conservation (in Italian: Rovina. Incompiuta. Chiesa Di San Michele Arcangelo a Brendola. Strumenti Di Conoscenza, Valorizzazione e Conservazione). Venezia: Marsilio; 2024, p. 107–24.
35. Della Torre S. I risultati del progetto CHERIE negli scenari post-pandemia: prospettive nell'azione del Cluster TICHE / The results of the CHERIE project in post-pandemic scenarios: perspectives in the action of the TICHE Cluster. IlCapitale Cult. 2020;11:553–9. https://doi.org/10.13138/2039-2362/2590.
36. Greco C, Rossi C, Della Torre S. Digitisation and cultural heritage between crisis and opportunity: the experience of the Egyptian Museum in Turin (in Italian: Digitalizzazione e patrimonio culturale tra crisi e opportunità: L'esperienza del Museo Egizio di Torino). Il Capitale Cult. 2020;11:197–212. https://doi.org/10.13138/2039-2362/2532.
37. http://cherie.cloud/index.php, (n.d.).
38. Delpozzo D, Appolonia L, Scala B, Adami A. Federated HBIM models for cultural heritage: survey model and conceptual model, in: The International Archives of the Photogrammetry, Remote Sensing and Spatial Information Sciences, 9th Intl. Workshop 3D-ARCH "3D Virtual Reconstruction and Visualization of Complex Architectures", 2–4 March 2022, Mantua, Italy. 2022; 191–197. https://doi.org/10.5194/isprs-archives-XLVI-2-W1-2022-191-2022.
39. Banfi FB, Brumana R, Roascio S, Previtali M, Roncoroni F, Mandelli A, Stanga C. 3D heritage reconstruction and scan-to-hbim-to-xr project of the tomb of Caecilia Metella and Caetani Castle, Rome, Italy, in: International Archives of the Photogrammetry, Remote Sensing and Spatial Information Sciences - 9th Intl. Workshop 3D-ARCH - 3D Virtual Reconstruction and Visualization of Complex Architectures, 2–4 March 2022, Mantua, Italy. 2022; 49–56. https://doi.org/10.5194/isprs-archives-XLVI-2-W1-2022-49-2022.
40. Oreni D, Brumana R, Torre SD, Banfi F. Survey, HBIM and conservation plan of a monumental building damaged by earthquake, in: The International Archives of the Photogrammetry, Remote Sensing and Spatial Information Sciences. 2017; 337–342. https://doi.org/10.5194/isprs-archives-XLII-5-W1-337-2017.
41. Sorbo E, Battista G, Beverari MD, Tosato M. The Scamozzi scenes and proscenium of the Teatro Olimpico in Vicenza: the process of evaluating the state of conservation for the project (in Italian: Scene scamozziane e proscenio del Teatro Olimpico di Vicenza: il processo di valutazione dello stato conservativo per il progetto) in: S. Della Torre, V. Russo (Eds.), Apparatus and Guideline Document for the Quality of Architectural Restoration Projects (in Italian: Apparati e Documento Di Indirizzo per La Qualità Dei Progetti Di Restauro Dell'architettura), III Convegno Della SIRA Società Italiana per Il Restauro Dell'Architettura "Restauro Dell'architettura. Per Un Progetto Di Qualità", Napoli, 15–16 Giugno 2023, Edizioni Quasar di S. Tognon srl, Roma. 2023; p. 610–618.
42. Bonini JA, Mandelli A, De Gennaro SM, Banfi F. BIM interoperability: open BIM-based workflow for heritage building information modelling (HBIM). A multidisciplinary approach based on advanced 3d tools and exchange formats, in: Proceedings of the Joint International Event 9th ARQUEOLÓGICA 2.0 & 3rd GEORES, Valencia (Spain). 26–28 April 2021, Universitat Politecnica de Valencia. 2021; 159–169. https://doi.org/10.4995/arqueologica9.2021.12104.
43. Ballarin M, Balletti C, Guerra F. Action cameras and low-cost aerial vehicles in archaeology, in: F. Remondino, M.R. Shortis (Eds.), Proceedings of SPIE "Videometrics, Range Imaging, and Applications XIII," SPIE. 2015; 952813. https://doi.org/10.1117/12.2184692.
44. Pignatelli O. Dendrochronological dating of some wooden elements in the Teatro Olimpico in Vicenza (in Italian: Datazioni dendrocronologiche di alcuni elementi lignei del Teatro Olimpico di Vicenza). In: Piana M, Soragni U, editors. Palladio: Materiali Tecniche Restauri Onore Di Renato Cevese (in Italian: Palladio: materiali, tecniche, restauri in onore di Renato Cevese). Venice: Marsilio; 2011. p. 23–6.
45. Goodell B, Qian Y, Jellison J. Fungal Decay of Wood: Soft Rot—Brown Rot—White Rot, in: Schultz T.P., Militz H., Freeman M.H., Goodell B., Nicholas D.D. (Eds.), Development of Commercial Wood Preservatives Efficacy, Environmental, and Health Issues, American Chemical Society, Washington DC; 2008, p. 9–31. https://doi.org/10.1021/bk-2008-0982.ch002.
46. Yona AMC, Žigon J, Matjaž P, Petrič M. Potentials of silicate-based formulations for wood protection and improvement of mechanical properties: a review. Wood Sci Technol. 2021;55:887–918. https://doi.org/10.1007/s00226-021-01290-w.
47. Lalli CG, Innocenti F. Artistic techniques of panel paintings from the 12th to the 16th century (in Italian: Tecniche artistiche di dipinti su tavola dal XII al XVI secolo). 2015. https://about.jstor.org/terms.
48. Cariati F, Rampazzi L, Toniolo L, Pozzi A. Calcium oxalate films on stone surfaces: experimental assessment of the chemical formation. Stud Conserv. 2000;45:180–188. https://doi.org/10.2307/1506764.
49. Del Monte M, Sabbioni C, Zappia G. The origin of calcium oxalates on historical buildings, monuments and natural outcrops. Sci Total Environ. 1987;67:17–39. https://doi.org/10.1016/0048-9697(87)90063-5.
50. Del Monte M, Sabbioni C. Chemical and biological weathering of an historical building: Reggio Emilia Cathedral. Sci Total Environ. 1986;50:165–82. https://doi.org/10.1016/0048-9697(86)90358-X.
51. Rampazzi L. Calcium oxalate films on works of art: a review. J Cult Herit. 2019;40:195–214. https://doi.org/10.1016/j.culher.2019.03.002.
52. Fang J, Xuan Y, Li Q. Preparation of polystyrene spheres in different particle sizes and assembly of the PS colloidal crystals. Sci China Technol Sci. 2010;53:3088–93. https://doi.org/10.1007/s11431-010-4110-5.
53. Derrick MR, Stulik D, Landry JM. Infrared Spectroscopy in Conservation Science. Scientific Tools for Conservation, The Getty Conservation Institute, Los Angeles; 1999.
54. La Rie D, René E. Ultraviolet radiation fluorescence of paint and varnish layers. PACT J Euro Study Group Phys Chem Math Tech Appl Archaeol 1986;13:91–108.
55. Lazzarini L, Borrelli E, Bouabdelli M, Antonelli F. Insight into the conservation problems of the stone building "Bab Agnaou", a XII cent. monumental gate in Marrakech (Morocco). J Cult Herit. 2007;8:315–22. https://doi.org/10.1016/j.culher.2007.02.002.
56. Antonelli F, Lazzarini L, Cancelliere S, Tesser E. Study of the deterioration products, gilding, and polychromy of the stones of the Scuola Grande di San Marco's façade in Venice. Stud Conserv. 2016;61:74–85. https://doi.org/10.1179/2047058415Y.0000000004.
57. Tomasini EP, Halac EB, Reinoso M, Di Liscia EJ, Maier MS. Micro-Raman spectroscopy of carbon-based black pigments. J Raman Spectrosc. 2012;43:1671–5. https://doi.org/10.1002/jrs.4159.
58. Bell IM, Clark RJH, Gibbs PJ. Raman spectroscopic library of natural and synthetic pigments (pre- approximately 1850 AD). Spectrochim Acta A Mol Biomol Spectrosc. 1997;53A:2159–79.
59. Sun J, Wu Z, Cheng H, Zhang Z, Frost RL. A Raman spectroscopic comparison of calcite and dolomite. Spectrochim Acta A Mol Biomol Spectrosc. 2014;117:158–62. https://doi.org/10.1016/j.saa.2013.08.014.
60. Ospitali F, Bersani D, Di Lonardo G, Lottici PP. 'Green earths': vibrational and elemental characterization of glauconites, celadonites and historical pigments. J Raman Spectrosc. 2008;39:1066–73. https://doi.org/10.1002/jrs.1983.
61. Burgio L, Clark RJH. Library of FT-Raman spectra of pigments, minerals, pigment media and varnishes, and supplement to existing library of Raman spectra of pigments with visible excitation. Spectrochim Acta A Mol Biomol Spectrosc. 2001;57:1491–521.
62. Tomasini E, Siracusano G, Maier MS. Spectroscopic, morphological and chemical characterization of historic pigments based on carbon. Paths for the identification of an artistic pigment. Microchem J. 2012;102:28–37. https://doi.org/10.1016/j.microc.2011.11.005.
63. Eastaugh N, Walsh V, Chaplin T, Siddall R. Pigment compendium a dictionary and optical microscopy of historical pigments. Oxford: Butterworth-Heinemann; 2008.
64. Newman R. Chromium Oxide Greens. Chromium oxide and hydrated chromium oxide' artists' pigments. In: FitzHugh EW (Ed). A handbook of their history and characteristics 3, 273rd–293rd ed. 1997; 273–293.
65. Cavallo G, Fontana F, Gonzato F, Guerreschi A, Riccardi MP, Sardelli G, Zorzin R. Sourcing and processing of ochre during the late upper Palaeolithic at Tagliente rock-shelter (NE Italy) based on conventional X-ray powder diffraction analysis, Archaeol. Anthropol Sci. 2017;9:763–75. https://doi.org/10.1007/s12520-015-0299-3.

66. Winter J. "Lead White" in Japanese Paintings, Studies in Conservation. 1981;26:89–101.
67. Harley RD. Artists' Pigments c.1600–1835. London: Butterworth Scientific; 1982.
68. Vandenabeele P, Moens L. Micro-Raman spectroscopy of natural and synthetic indigo samples. Analyst. 2003;128:187–93. https://doi.org/10.1039/b209630g.
69. Spring M. New insights into the materials of fifteenth- and sixteenth-century Netherlandish paintings in the National Gallery, London. Herit Sci. 2017. https://doi.org/10.1186/s40494-017-0152-3.
70. Vitorino T, Casini A, Cucci C, Melo MJ, Picollo M, Stefani L. Non-invasive identification of traditional red lake pigments in fourteenth to sixteenth centuries paintings through the use of hyperspectral imaging technique. Appl Phys A Mater Sci Process. 2015;121:891–901. https://doi.org/10.1007/s00339-015-9360-4.
71. Doktor R. Painting techniques. 1938. https://www.jstor.org/stable/771606.
72. Caforio L, Fedi M, Liccioli L, Salvini A. The issue of contamination by synthetic resins in radiocarbon dating: the case of a painting by Ambrogio Lorenzetti. Procedia Chem. 2013;8:28–34. https://doi.org/10.1016/j.proche.2013.03.005.
73. Piovesan R, Tesser E, Maritan L, Zaccariello G, Mazzoli C, Antonelli F. Mapping of stones and their deterioration forms: the Clock Tower, Venice (Italy). Herit Sci. 2023. https://doi.org/10.1186/s40494-023-00909-4.
74. ICOMOS, ISCS, ICOMOS-ISCS. Illustrated glossary on stone deterioration patterns, XV, ICOMOS, Paris, France; 2008.

Publisher's Note